Brain, Behavior, and Immunity 69 (2018) 515–531

Contents lists available at ScienceDirect

Brain, Behavior, and Immunity

journal homepage: www.elsevier.com/locate/ybrbi

Full-length Article

A new focal model resembling features of cortical pathology of the progressive forms of multiple sclerosis: Influence of innate immunity

Berenice Anabel Silva [a,b], María Celeste Leal [b], María Isabel Farías [b], Juan Carlos Avalos [c], Cristina Hilda Besada [d], Fernando Juan Pitossi [b], Carina Cintia Ferrari [a,b,*]

[a] Institute of Basic Science and Experimental Medicine (ICBME), University Institute, Italian Hospital, Buenos Aires, Argentina
[b] Leloir Institute Foundation, Institute for Biochemical Investigations of Buenos Aires, (IIBBA, CONICET), Buenos Aires, Argentina
[c] Neurology Department, Italian Hospital, Buenos Aires, Argentina
[d] Neuroimaging Unit, Italian Hospital, Buenos Aires, Argentina

ARTICLE INFO

Article history:
Received 31 August 2017
Received in revised form 10 January 2018
Accepted 19 January 2018
Available online 31 January 2018

Keywords:
Progressive multiple sclerosis
Animal model
Innate immunity
Cytokines
Interleukin 1β

ABSTRACT

Multiple sclerosis (MS) is an inflammatory and demyelinating disease of unknown aetiology that causes neurological disabilities in young adults. MS displays different clinical patterns, including recurrent episodes with remission periods ("relapsing-remitting MS" (RRMS)), which can progress over several years to a secondary progressive form (SPMS). However, 10% of patients display persistent progression at the onset of disease ("primary progressive MS" (PPMS)). Currently, no specific therapeutic agents are available for the progressive forms, mainly because the underlying pathogenic mechanisms are not clear and because no animal models have been specifically developed for these forms. The development of MS animal models is required to clarify the pathological mechanisms and to test novel therapeutic agents.

In the present work, we overexpressed interleukin 1 beta (IL-1β) in the cortex to develop an animal model reflecting the main pathological hallmarks of MS. The treated animals presented with neuroinflammation, demyelination, glial activation, and neurodegeneration along with cognitive symptoms and MRI images consistent with MS pathology. We also demonstrated the presence of meningeal inflammation close to cortical lesions, with characteristics similar to those described in MS patients. Systemic pro-inflammatory stimulation caused a flare-up of the cortical lesions and behavioural symptoms, including impairment of working memory and the appearance of anxiety-like symptoms.

Our work demonstrated induced cortical lesions, reflecting the main histopathological hallmarks and cognitive impairments characterizing the cortical pathology described in MS patients with progressive forms of the disease.

1. Background

Multiple sclerosis (MS) is a chronic immune-mediated demyelinating disease of unknown aetiology characterized by neuroinflammation, demyelination and axonal degeneration, leading to loss of sensory, motor, autonomic and cognitive functions, according to the location of the central nervous system (CNS) lesions. MS represents one of the most important causes of disability among young adults (between 20 and 45 years old), resulting in important socio-economic impacts in developed countries (Denic et al., 2011; Martinez Yelamos et al., 1999). MS is a very heterogeneous disease that displays different clinical courses, including episodes with periods of relapse and remission of symptoms ("relapsing-remitting MS" (RRMS)). RRMS can progress to a secondary progressive form (SPMS); however, some patients experience persistent progression from the onset of the disease ("primary progressive MS" (PPMS)). Additionally, according to new imaging findings, progressive disease (secondary and primary) can be active (with or without progression) or inactive (with or without progression; the latter case is called "stable disease") (Lublin et al., 2014). Currently, there are anti-inflammatory and immunomodulatory treatments that are beneficial for RRMS, but they are ineffective for SPMS (Losy, 2013; Watzlawik et al., 2010). However, there is only one anti-inflammatory treatment for PPMS, which was recently approved (Frampton, 2017). Although the treatment of RRMS provides temporary effectiveness because it reduces the annualized

* Corresponding author at: Institute of Basic Science and Experimental Medicine (ICBME), University Institute, Italian Hospital, Potosi 4240, (C1199ABB), CABA, Buenos Aires, Argentina.
E-mail address: carina.ferrari@hospitalitaliano.org.ar (C.C. Ferrari).

https://doi.org/10.1016/j.bbi.2018.01.010
0889-1591/

relapse rate, patients experience side effects, relapses or evolution to progressive MS stages (Ontaneda and Fox, 2015; Watzlawik et al., 2010).

Cortical demyelinated lesions are considered a key feature of PPMS and SPMS, but they are rare in RRMS (Kutzelnigg et al., 2005; Popescu and Lucchinetti, 2012). These lesions have peculiar inflammatory and demyelinating hallmarks, with an absence of blood-brain barrier (BBB) disruption, differential inflammatory processes, reactive microglia, neurodegeneration and meningeal inflammation. These observations suggest different immunopathogenic mechanisms of the PPMS and SPMS forms compared with the RRMS form, potentially because the inflammatory environment in progressive MS favours the retention of inflammatory cells within lesions (Choi et al., 2012; Howell et al., 2011; Lassmann et al., 2012; Magliozzi et al., 2007; Serafini et al., 2004).

The main challenge in modelling SPMS and PPMS is the impossibility of replicating the chronicity and cortical injury patterns of these forms of MS, which differ from those of RRMS. Furthermore, most models do not reflect the irreversibility that characterizes the progressive forms of MS (Fox et al., 2012). Experimental animal models that have conclusively demonstrated chronic demyelination, neurodegeneration, autoimmune inflammatory processes, and glial activation, which occur in progressive MS, are required (Fox et al., 2012). Several animal models have been developed in recent years to mimic these forms of the disease. These models are based on myelin oligodendrocyte glycoprotein (MOG) immunization of rats, along with focal injection of cytokines (TNF-α and IFN-γ). These models reflect different aspects of MS pathology, but the chronicity and behavioural symptoms vary according to the model. Interestingly, none of the described models of cortical lesions can be visualized by MRI (see Table 1).

In recent years, studies of the influence of environmental factors, both on the risk of MS and on the progression of the disease, including systemic infections, vitamin D levels, salt intake, smoking, obesity, and the composition of the microbiota, have become relevant (Ascherio and Munger, 2016; Montalban and Tintore, 2014; Ramanujam et al., 2015). These environmental factors generate a pro-inflammatory peripheral environment with increased levels of circulating cytokines. Until now, few studies have described the effects of this pro-inflammatory environment on the cerebral cortices of MS patients (Gacias et al., 2016; Hoban et al., 2016; Mashayekhi and Salehi, 2016).

IL-1β is a prototypic pro-inflammatory cytokine. The functional relevance of IL-1β expression has been demonstrated in both MS pathology and many MS animal models. IL-1β is present in MS lesions, and it exerts its cytotoxic action either by a direct effect on CNS cells or by a secondary effect on leukocyte recruitment (Argaw et al., 2006; Howe et al., 2006; Kitic et al., 2013; Zeis et al., 2008). The presence of IL-1β and its ability to induce neutrophil recruitment have been demonstrated during the onset of EAE and in cuprizone experimental models (Liu et al., 2010; Soulika et al., 2009). Additionally, elevated numbers of primed neutrophils have been found to contribute to pathology in MS patients (Naegele et al., 2011).

The aim of the present paper was to study the effect of the long-term expression of IL-1β in the prefrontal cortices of adult rats and the effect of a pro-inflammatory peripheral stimulus on the progression of chronic cortical lesions. According to histological, imagenological, and behavioural parameters, we developed an experimental animal model that represents most of the characteristics of the cortical lesions that appear in progressive stages of MS, such as cortical neuroinflammation, neurodegeneration, meningeal inflammation, and cognitive impairment.

2. Materials and methods

2.1. Adenoviral vectors

Adenoviral vectors expressing the human interleukin 1β gene (AdIL-1β) or the reporter gene β-galactosidase (Adβgal) as a control were generated as described previously (Ferrari et al., 2004). Stocks were obtained by large scale amplification in HEK293 cells, purified in double caesium chloride gradients, and quantified by plaque assay (final titters: Adβgal = 8.41. 10^{11} infective particles/ml; AdIL-1β = 1.1. 10^{11} infective particles/ml). Stocks had <1 ng/ml endotoxin, which was assayed with E-TOXATE reagents (Sigma, St. Louis, MO, USA). Viral stocks were free of autoreplicative particles as assessed by PCR. Adβgal was kindly provided by Dr. J. Mallet (Hospital Pitie Salpetriere, Paris, France).

Table 1
Animal models of cortical pathology of MS.

Animal/ immunization	Focal injection	Pathology	Recovery	Strengths	Weakness	References
Lewis Rat/ MOG	1 μl de 250 ng TNF α + 150 U IFN (prefrontal cortex)	-Cortical inflammation (ED1, CD4, CD8) and demyelination -Neuronal apoptosis (maximum at 7 dpi)	14 days	-Adaptive immunity -Neuronal loss	-Acute -No MRI studies -No behavioural tests	Merkler et al. (2006)
Dark Agouti Rat/MOG	1. 25 μg TNFα + 75 ng IFN (subarachnoid space)	-Meningeal inflammation, subpial demyelination, microglia activation. -No neuronal loss (maximum at 7 dpi)	14 days	-Adaptive immunity -Meningeal Inflammation	-Acute -Only subpial demyelination -No MRI studies -No neuronal loss -No behavioural test	Gardner et al. (2013)
Dark Agouti Rat/MOG	500 μg/ml TNF α + 300 U IFNγ (catheter into the cortex)	-Cortical inflammation and demyelination -Meningeal inflammation -Neuronal apoptosis (maximum at 15 dpi)	30 days	-Chronicity -Meningeal inflammation	-The use of catheter into the cortex -Undetectable lesions by MRI -No behavioural tests	Ucal et al. (2017)
C57BL/6J Mice/MOG	50 ng TNFα + 50 ng IFNγ (motor cortex)	-Inflammatory infiltrate (CD3+, NK + . macrophages) -Subpial and perivascular demyelination Perivascular APP++ (maximum at 5 dpi) -Motor deficiencies	20–40 days	-Adaptive immunity -Axonal loss -Chronicity	-No MRI studies -No behavioural tests	Lagumersindez-Denis et al. (2017)

2.2. Animals and injections

Adult male Wistar rats (Jackson Laboratory, Bar Harbor, ME, USA), bred for several generations in the Leloir Institute Foundation and in ICBME's animal facility, were used in all of the experiments. The animals were housed under controlled temperature conditions (22 °C ± 2 °C), with food and water provided ad libitum and a 12:12 dark:light cycle with lights on at 08.00 h. All of the surgical procedures and euthanasia were conducted in full compliance with NIH and internal Institute Foundation Leloir and Italian Hospital guidelines and were approved by the Institutional Review Board "Cuidado y Uso de Animales de Laboratorio (CICUAL-FIL)" and "Comité de Ética y Protocolos de Investigación (CEPI- HIBA)", respectively.

For stereotaxic injections, the animals were anaesthetized with ketamine chlorhydrate (80 mg/kg) and xylazine (8 mg/kg). Adenoviral vectors were delivered via a finely drawn, graduated capillary into the left prefrontal cortex (bregma, +1.6 mm; lateral, +2.5 mm; ventral, −1.6 mm) (Paxinos and Watson, 1986). Human IL-1β- and βgal-expressing vectors were diluted in sterile Tris-HCl buffer (Tris-HCl 10 mM, $MgCl_2$ 1 mM, pH 7.8) to a concentration of 1×10^6 infective particles/μl. Previous work published by our laboratory (Ferrari et al., 2004; Murta et al., 2012, 2015) and pilot studies have shown that this dose is the minimum for both AdIL-1β and Adβgal that provides long-term expression of the transgenes with a minimum inflammatory response to the control vector. The volume of the intracortical injection was 1 μl, which was infused over a 5-min period, with the capillary remaining in place for another minute to minimize reflux. All of the surgical procedures were conducted in the morning to avoid possible circadian variations in cytokine expression.

For peripheral injections, the animals were briefly anaesthetized with isoflurane, and adenoviruses expressing IL-1β or βgal were injected intravenously (iv) at doses of 1.36×10^9 infective particles/rat. The final volume of injection was 600 μl: 300 μl of the adenovector solution (in sterile 10 mM Tris-HCl, 1 mM $MgCl_2$-n, pH = 7.8), followed by 300 μl of saline solution. All iv administrations were performed between 2 p.m. and 5 p.m.

The adenoviruses were initially administered in the periphery at day 21 after injection of adenovirus into the cortex. Five days after the iv injection, a blood smear was performed to confirm the effectiveness of the pro-inflammatory systemic stimulus according to Murta et al. (2015). A significant increase in the number of PMNs in AdIL-1β endovenously injected (AdIL-1βiv) animals, along with a consequent decrease in the lymphocyte population, was considered a sign of inflammation. For all of the experiments in this study, AdIL-1βiv-mediated changes in the blood formula were significantly different from those observed in Adβgal iv-injected animals. The animals were sacrificed 7 and 30 days after the systemic stimuli, and their brains were processed for histological and molecular analyses.

2.3. Behavioural tests

2.3.1. Open field

Spontaneous locomotor activity and anxiety-like behaviour were quantified in adult rats (n = 10–12/group) using an open field arena and a wooden box of 1 m × 1 m with the floor divided into 16 squares. Line crossings, rears and climbing were scored for 5 min. A line crossing was counted when all four paws crossed the square lines. Rearing was scored when the animals raised both front paws from the floor. Time spent in both central and peripheral squares was also measured. Faecal boli were also counted (Prut and Belzung, 2003).

2.3.2. Novel object recognition test

To evaluate short-term memory, we performed the novel object recognition test. The rats (n = 10–12/group) were placed in the arena for 5 min with two identical objects. After 2 h, the rats were re-introduced into the arena, with a new object replacing on previous object over 3 min. The time (measured by seconds) until the animal came into contact with the objects with its nose was recorded and quantified as the novel object exploration time and discrimination index (DI). The DI was calculated as described previously (Antunes and Biala, 2012):

$$\mathrm{DI} = \frac{\text{Time in novel object} - \text{Time in familiar object}}{(\text{Time in novel object} + \text{Time in the familiar object})}$$

Combinations of the objects and their locations differed among the animals such that right-left preference could be avoided.

2.4. Magnetic resonance imaging

Brain MRI was performed under anaesthesia with ketamine chlorhydrate (80 mg/kg) and xylazine (8 mg/kg). The animals (n = 4/group) were scanned in a 3.0 T MRI system (Philips Ingenia) using a human wrist coil (Wrist 8-ch, Invivo, Gainesville, FL, USA) for signal reception. The animals were placed in the prone position, with their heads and upper spines inside the coil with three-dimensional (3D) imaging volumes in the transverse orientation.

The MRI protocol included T1-weighting with a slice thickness of 1 mm (voxel size 0.34, FOV 60, TR 600 ms, TE 20 ms). For the detection of lesions, T2-weighted MRI was performed with a slice thickness of 1 mm and axial and coronal sequences (voxel size 0.35, FOV 70, TE 140 ms, TR 1174 ms). To detect acute inflammation, T1-weighted MRI was repeated at 3 and 6 min after intravenous application of 1 ml of gadolinium-based contrast agent (gadoterate meglumine-Dotarem®).

On a separate workstation, every contrast-enhancing lesion or hyperintensity on T2-weighted images was analysed by an experienced neuroradiologist in a blinded manner. Moreover, enhancement of the cortical lesions was assessed as present or absent.

2.5. Histology

The animals (n = 8–10/group) were deeply anaesthetized as previously described (Murta et al., 2012; Murta et al., 2015) and were transcardially perfused with heparinized saline, followed by ice-cold 4% paraformaldehyde in 0.1 M phosphate buffer (PB) with a pH of 7.2. Brains were dissected and placed in the same fixative overnight at 4 °C and cryoprotected in 30% sucrose 0.1 M PB solution. Then, the brains were frozen in isopentane and cut using a cryostat into 40-μm serial coronal sections through the left prefrontal cortex. Sections were mounted on gelatine-coated slides and stained with Cresyl Violet to assess the general nervous tissue integrity and inflammation and with Red Oil O to evaluate the myelin. For immunohistochemistry, sections were stored in cryoprotective solution at −20 °C until needed.

2.6. Immunohistochemistry

Free-floating sections were rinsed in 0.1% Triton in 0.1 mol/L PB, blocked in 1% donkey serum for 45 min, and then incubated overnight at 4 °C with primary antibodies diluted in blocking solution. The list of antibodies is provided in Table 2. After three 10-min washes with 0.1 mol/L PB, the sections were incubated with indocarbocyanine (Cy3) or cyanine Cy2 (Cy2)-conjugated donkey anti-rabbit or anti-mouse antibody, respectively (1:250; Jackson ImmunoResearch Laboratories Inc., West Grove, PA, USA) for 2 h

Table 2
Antibody list.

Antibody	Origin	Target	Dilution	Antigen Retrieval	Source
MHC II	Mouse	MHC Class II restricted macrophages, dendritic cells and B- cells	1:200	no	Serotec
GFAP	Rabbit	Glial fibrillary acidic protein	1:700	no	Dako
APP	Human	Amyloid precursor protein	1:100	yes	Invitrogen
NeuN	Mouse	Neuron-specific nuclear protein	1:1000	no	EMD Millipore
Casp3, Active	Rabbit	Apoptotic cells	1:200	no	Neuromics
CD45RC	Mouse	Pre B lymphocytes, B cells, T cells	1:100	no	Serotec
CD8	Mouse	MHC Class I restricted T-cells	1:1000	no	Serotec
CD4	Mouse	MHC Class I restricted T-cells	1:1000	no	Abcam
CD39	Guinea Pig	B cells, T cells, NK cells	1:50	no	Neuromics
CD20	Human	Cd20 receptor in B cells	1:3000	yes	Ventana, Roche
CD23	Human	Cd23 receptor in follicular dendritic cells	1:5000	yes	Ventana, Roche
MBP	Rabbit	Myelin basic protein	1:200	no	Kindly provided by Páez P, School of Medicine and Biomedical Sciences, University at Buffalo
ED1	Mouse	Pan-macrophage marker	1:100	no	Serotec

at room temperature, rinsed in 0.1 mol/L PB and mounted in Mowiol (Calbiochem, San Diego, CA, USA). Digital images were obtained in a Zeiss LSM 510 laser scanning confocal microscope equipped with a krypton-argon laser.

2.7. Electron microscopy

Anaesthetized animals ($n = 3$/group) were intracardially perfused with a modified saline solution (0.8% NaCl, 0.8% sucrose, 0.4% glucose), followed by a fixative consisting of 2% glutaraldehyde and 2% paraformaldehyde in 0.1 mol/L cacodylate buffer (CB) (pH 7.2). The 1-mm^3 cortex samples were then immersed in the same fixative at 4 °C overnight. The tissue was stored in 0.1 mol/L CB with 0.2 mol/L sucrose. After 5-min washes in CB, they were post-fixed in OsO_4 in CB for 1 h, washed in buffer, dehydrated in an ethanol series, cleared in acetone, and embedded in Spurr resin. Semi-thin and ultra-thin sections were cut using a Sorvall-Porter-Blum ultramicrotome. The semi-thin sections were stained with toluidine blue, and the ultra-thin sections were double-stained with uranyl acetate and lead citrate. Ultra-thin sections were examined using a JEOL 1200EX2 electron microscope (Facultad de Veterinaria, Universidad de La Plata).

2.8. Assessment of blood–brain barrier permeability

For the evaluation of BBB integrity, the animals ($n = 8$–10/group) were injected intravenously with 10^4 U/kg of type II horseradish peroxidase (HRP, Sigma, St. Louis, MO) 30 min before perfusion. The animals were then perfused with Karnovsky's fixative, and their brains were processed as previously described. HRP was detected in free-floating sections using the modified Hanker-Yates method (Perry and Linden, 1982).

2.9. Quantitative analysis

The lesion volume was calculated using every sixth 40-μm-thick serial section of the entire ipsilateral left prefrontal cortex, according to the anatomical landmarks defined by Paxinos and Watson (1986).

Photographs of all of the sections were obtained using a Nikon Eclipse E600 microscope and a CX900 camera (MicrobrightField Inc., USA) under a 4x magnification objective. The area of one set of serial sections was used for inflammation analysis (Cresyl Violet), and the adjacent group of serial sections was used to evaluate the demyelinating volume (Red Oil-O). The inflammatory and the demyelinated area were delineated and measured using ImageJ software (Media Cybernetics, Silver Spring, MD, USA). All of the measurements were obtained in a blinded manner. The inflammatory and demyelinating averages (IA and DA, respectively) were calculated for each animal, and the average volumes of inflammation and demyelination (IV and DV, respectively) were estimated by multiplying the IA/DA by the width of the section (0.04 mm) and by the total number of sections obtained for the entire left prefrontal cortex.

For MHC II-positive cell quantification, a 20× objective was used, and one image of the ipsilateral cortex was obtained from each section. The laser power, gain, and offset conditions were kept constant for the acquisition of all of the images. Approximately 12 fields were quantified for each animal using the Zeiss LSM Image Browser. The total number of positive cells was normalized to the total area counted for each animal. To quantify GFAP-positive cells, 20× objective images of the ipsilateral cortex from each section were obtained under the same laser power, gain, and offset conditions, and the GFAP intensity was calculated using ImageJ software.

2.10. RNA isolation, reverse transcription, and real-time PCR

The animals ($n = 5$–6/group) were decapitated, their brains were quickly removed, and the prefrontal cortex pieces were dissected, snap-frozen in liquid nitrogen, and stored at −80 °C. RNA was prepared by homogenizing the tissue using the GenElute Mammalian Total RNA Miniprep kit (Sigma, St. Louis, MO). Samples were treated with DNAase I to eliminate possible DNA contamination (On-Column DNase I Digestion, Sigma). RNA was quantified with a Nanodrop (Nanodrop Technologies, Wilmington, DE, USA), and 200 ng of total RNA were reverse-transcribed according to the manufacturer's protocol (Superscript II, Invitrogen, Life Technologies, Carlsbad, CA, USA) using oligo-dT primers. As a control for genomic contamination, a sample without reverse transcriptase was included in each PCR analysis. Relative quantification was performed by real-time PCR using the SYBR-green I fluorescence method and ROX as a passive reference dye. Stratagene MxPro TM QPCR Software and Stratagene Mx3005P equipment were used (Agilent Technologies, Santa Clara, CA, USA). TATA box binding protein (TBP) was used as a housekeeping gene because its expression is not altered by the treatment (forward: 5′-ACCGTGAATCTTGGCTGTAA, reverse: 5′-CCGTGGCTCT CTTATTCTCA). All of the samples were assessed in triplicate. Specificity was controlled by melting curves and agarose gels. To calculate the efficiency, LinReg PCR was used (Cikos et al., 2007). The primers for the studied cytokines were as follows: IL-1β (forward: 5′-TCCATGAGCTTTGTACAAGG, reverse: 5′-GGTGCTGATGTAC CAGTTGG), IL-6 (forward: 5′-GCCAGAGTCATTCAGAGCAATA,

reverse: 5′-GTTGGATGGTCTTGGTCCTTAG), and TNF-α (forward: 5′-GTAGCCCACGTCGTAGCAAA, reverse: 5′-AAATGGCAAATCGG CTGACG).

2.11. Statistical analysis

The results are expressed as the mean ± SEM. All of the experiments were analysed by parametric one-way ANOVA or two-way ANOVA, followed by Bonferroni's multiple comparison test as the post hoc test. Student's unpaired *t*-test was used when comparing experiments with only two groups. Variables were tested for normality (Kolmogorov-Smirnov) and variance homogeneity (Bartlett's test) (Scheirer et al., 1976). The level of statistical significance was set at $p < 0.05$. For clarity, statistical analyses of each test are addressed in each figure legend. Statistical tests were performed using GraphPad Prism software, version 6.00 for Windows (GraphPad Software, San Diego, CA, USA).

3. Results

3.1. Central and peripherally stimulated lesions are associated with cognitive impairment and anxiety-like symptoms

To study the effect of the long-term expression of IL-1β on the prefrontal cortices of adult rats and the effects of the pro-inflammatory peripheral stimulus on the progression of ongoing cortical lesions, the animals were centrally injected with either AdIL-1β (CI) or Adβgal (control) (CC) in the cortex. The animals were studied at 15, 21, and 30 days post-injection (dpi) (Fig. 1A). The animals that had previously received intracortical injection with either AdIL-1β or Adβgal were then peripherally injected at 21 dpi. According to this experimental design, four experimental groups were generated: centralAdIL-1β/peripheralAdIL-1β (CI/PI); centralAdIL-1β/peripheral Adβgal (CI/PC); central Adβgal/peripheralAdIL-1β (CC/PI); and central Adβgal/peripheral Adβgal (CC/PC). These four groups were analysed at 7 (21 + 7) and 30 (21 + 30) days after the peripheral injections (Fig. 1C). Previously published results from our laboratory (Murta et al., 2015; Pott Godoy et al., 2008; Pott Godoy et al., 2010) revealed that a maximum systemic effect of the iv-administered AdIL-1β was achieved 5 days after injection. Briefly, peripheral treatment efficiency was checked by analysing the proportions of peripheral blood lymphocytes (Lymph) and polymorphonuclear neutrophils (PMNs) 5 days after the iv injection. The peripheral AdIL-1β-injected animals exhibited a significant increase in the number of PMNs, together with a consequent decrease in the lymphocyte population, which was significantly different from the effects observed in the peripheral Adβgal-injected animals (Fig. 1D). All of the animal groups were periodically monitored, and no clinical symptoms, according to the standard Experimental Autoimmune Encephalomyelitis (EAE) score, were observed, indicating that the welfare of the animals was consistent with the high standards of the ethical guidelines for animals and were acceptable compared to other MS models, especially EAE. Additionally, the experimental animals did not show signs of ongoing disease. They presented with normal fur, activity, movement, and food consumption.

The CI-injected animals exhibited increased mRNA expression of IL-1β, which peaked at 15 dpi, consistent with the maximum peaks for both inflammation and demyelination. Its expression decreased until the last time point studied, 30 dpi (Fig. 1B). The CI/PI 21 + 7 and 21 + 30 groups exhibited strong increases in IL-1β expression (Fig. 1E). IL-1β expression was sustained for 50 days, demonstrating the chronicity of the proposed model.

The chronic expression of IL-1β in the prefrontal cortex induced short-term memory impairment, as evidenced by a significant decrease in time contacts with the novel object in the Novel Object Recognition (NOR) test at only 15 dpi in CI animals (Fig. 2A). However, analysis of the discrimination index (DI) demonstrated that both CI 15 dpi and CI 21 dpi animals displayed significant differences from CC control animals (Fig. 2B). The DI recovered in CI 30 dpi animals, as evidenced by an increase in this DI compared with the CI 15 dpi animals (Fig. 2B). No anxiety-like symptoms were observed at any time point studied when the animals received only central injections (data not shown).

The animals that were also peripherally stimulated with AdIL-1β (CI/PI) exhibited short-term memory impairment compared with the control Adβgal animals (CI/PC), as evidenced by reduced time with the novel object in the NOR test at both time points studied (21 + 7 and 21 + 30), demonstrating that cognitive impairment persisted for at least 51 days (Fig. 2C). The DI also showed an impairment of working memory, as demonstrated by a decreasing index at both time points studied (21 + 7 and 21 + 30) (Fig. 2D). It is interesting to note that there were no significant differences in symptoms for the CI/PI group at the two time points studied (21 + 7 and 21 + 30), demonstrating the chronicity of the cognitive impairment evidenced by DI (Fig. 2C and D). The control CC/PI animals did not display any symptoms on any of the studied tests.

To evaluate exploratory activity and anxiety-like symptoms, we performed the open field test. Exploratory activity was significantly decreased in CI/PI animals compared with CI/PC animals at both time points (21 + 7 and 21 + 30) (Fig. 2H). In particular, CI/PI animals exhibited more anxiety-like symptoms than CI/PC animals at both time points (Fig. 2E–G). These symptoms were shown as a significant decrease in time in the centre in CI/PI animals, compared with CI/PC control animals (Fig. 2G). Additionally, CI/PI animals had fewer rearings and an increased number of faecal boli compared with CI/PC animals (Fig. 2E and F). Because no significant differences were found between CI/PI 21 + 7 and 21 + 30 (Fig. 2E–H), these behavioural tests demonstrated that the anxiety-like symptoms persisted for at least 50 days after the central injection of AdIL-1β, when the animals received a peripheral inflammatory stimulation.

No anxiety-like symptoms were observed in control CC/PI animals on any of the performed tests (Fig. 2E–H).

3.2. Inflammation and glial activation

Long-term expression of IL-1β in the cortex induced inflammation characterized by the considerable recruitment of neutrophils and, to a reduced extent, macrophages. This infiltration was accompanied by tissue disorganization and oedema. The neuroinflammation peaked at 15–21 dpi, and the lesions were restored by 30 dpi (Fig. 3A and Suppl. Fig. 1). As the lesions evolved, the inflammatory infiltrate was modified and showed fewer neutrophils and an increasing number of macrophages. Additionally, these lesions induced the activation of astroglia and microglial cells, which were observed as increased GFAP and MHC-II expression, respectively (Fig. 3B and C and Suppl. Fig. 1).

The peripheral pro-inflammatory stimulus resulted in a flare-up of the chronic cortical lesions in experimental animals (CI/PI), compared with control animals (CI/PC) (Fig. 3D–F). The inflammatory infiltrate in CI/PI 21 + 7 animals was mostly composed of neutrophils and macrophages, but the CI/PC animals presented inflammatory infiltration of macrophages with sparse neutrophils (Suppl. Fig. 2). Indeed, neutrophil numbers were statistically increased in CI/PI compared with CI/PC animals at 21 + 7 (Suppl. Fig. 2A). No neutrophils could be observed in CI/PI 21 + 30 animals. The inflammatory volume was exacerbated in both CI/PI 21 + 7 and 21 + 30 animals, compared with CI/PC animals. However, although the inflammatory volume significantly decreased in CI/PI 21 + 30 com-

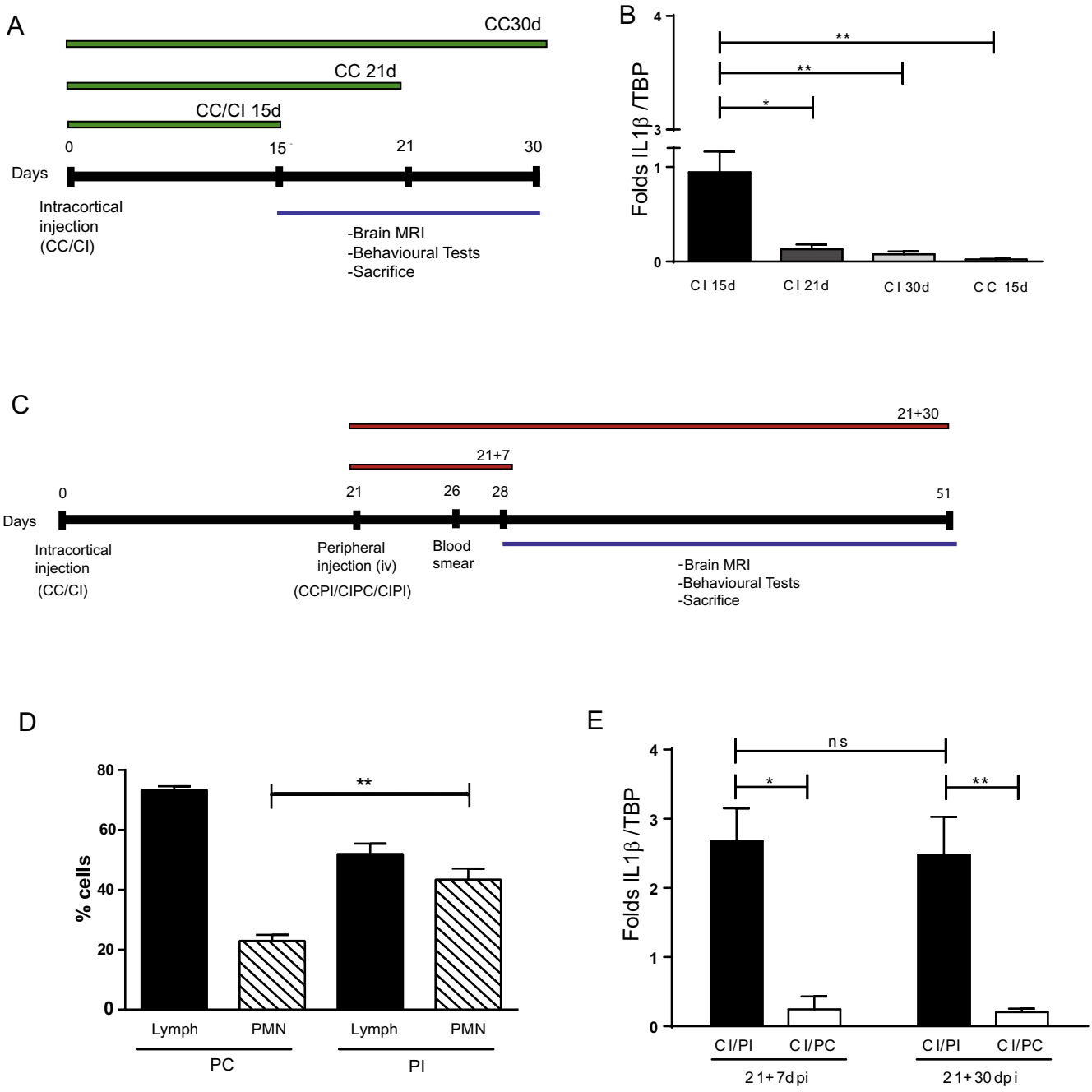

Fig. 1. Experimental designs, timelines and assessment of the models. A and B. Central injection experiments. A. Animals received an intracortical injection either with AdIL-1β or Adβgal (CI and CC, respectively). Behavioural, MRI and histopathological studies were performed at 15, 21 and 30 days post injection (dpi). B. Central injection of AdIL-1β induced IL-1β in the cortex of experimental animals, measured by real-time PCR. CI animals exhibited a maximum expression at 15dpi (one way ANOVA, Tukey post hoc test). C–E. Peripheral injection experiments. Animals received a central inflammatory stimulus at day 0, and a peripheral injection of AdIL-1β (PI) or Adβgal (PC) after 21 days (CI/PI and CI/PC). The studies were performed at 7 or 30 days after the peripheral stimulation (21 + 7dpi and 21 + 30dpi). D. Blood smears were performed 5 days after the peripheral injection. Representative blood smear counts as a control for the effectiveness of the peripheral stimulus (Unpaired *t* test) (*n* = 6/group). This control was repeated in every experiment performed throughout the present work. E. The peripherally stimulated lesions showed an increased IL-1β expression in the cortex at both time points studied by real time PCR (2 way-ANOVA, Bonferroni post hoc test). *n* = 5–6/group for real time PCR. ns $p \geq 0.05$, $^{*}p$ 0.01–0.05, $^{**}p$ 0.001–0.01.

pared with CI/PI 21 + 7, the inflammation persisted for 50 days compared with the control group (Fig. 3D). No inflammatory lesions were observed in CC/PI 21 + 7 control animals (Fig. 1D), demonstrating that Adβgal did not induce inflammatory lesions despite receiving a pro-inflammatory stimulus (Suppl Fig. 2E).

Peripheral stimulation with AdIL-1β resulted in the flare-up and activation of astroglia and microglia in CI/PI 21 + 7 and 21 + 30 animals, as demonstrated by the presence of MHC-II and GFAP (Fig. 3G–L). The MHC-II-positive microglial cells were types 3 and 4 according to the modified Kreutzberg classification (Kreutzberg, 1996; Pott Godoy et al., 2008) (Fig. 3K), and they were distributed along the parenchyma and perivascular region in CI/PI animals. Type 4 MHC-II-positive cells were also observed surrounding the blood vessels in CI/PC animals. Additionally, ED1-positive cells were observed in both CI/PI and CI/PC animals with the same distribution as described for MHC-II, demonstrating the phagocytic activity of these cells (Suppl Fig. 2). There were no differences between the CI/PI 21 + 7 and CI/PI 21 + 30 groups, suggesting that

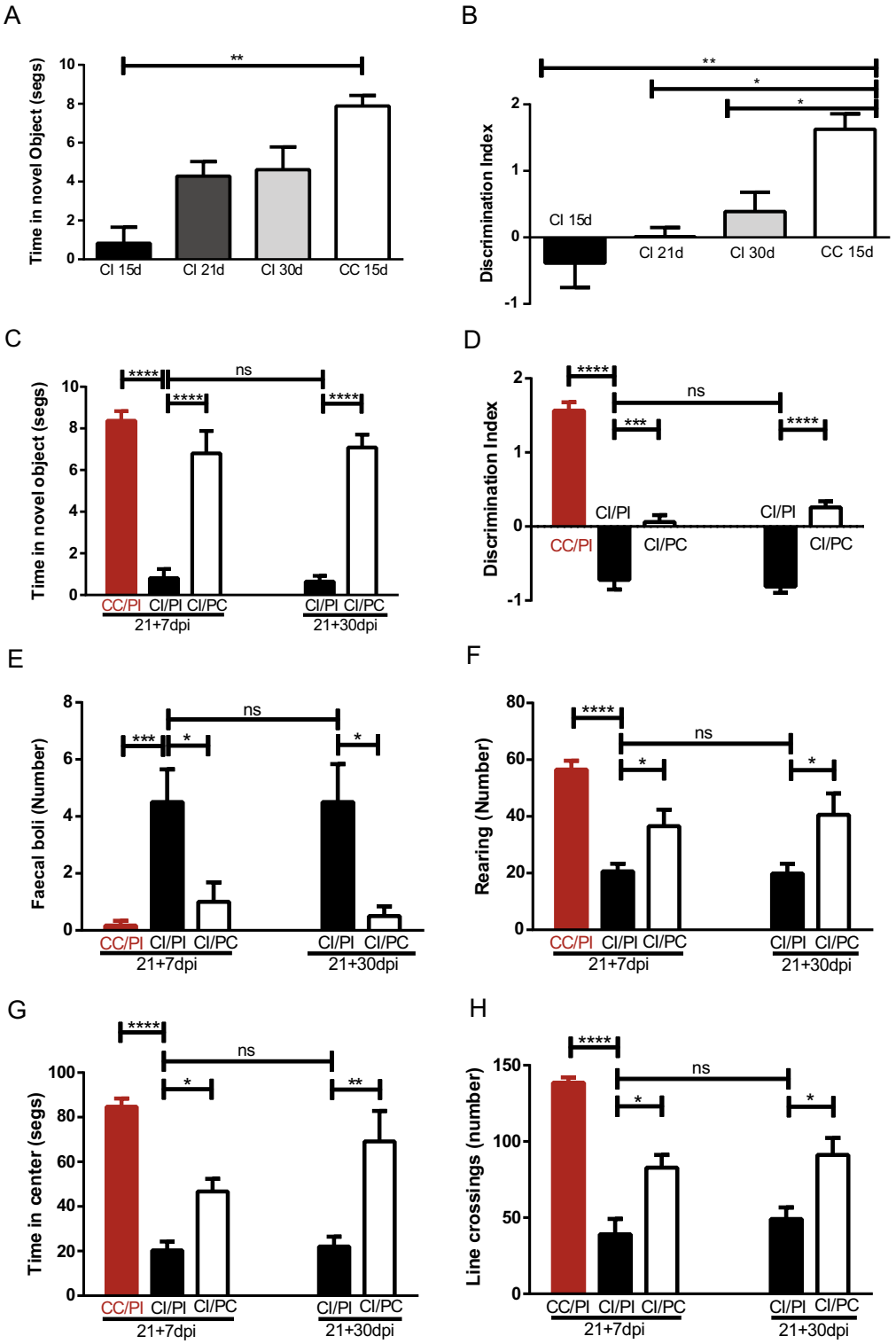

Fig. 2. Behavioural tests. A and B. The chronic expression of IL-1β in the prefrontal cortex induces short-term memory impairment, as evidenced by a significantly decrease of time contacts with the novel object in the Novel Object Recognition Test (NOR) only on day 15 dpi in CI animals (A). B The analysis of the discrimination index (DI) demonstrated that CI 15, 21 y 30 dpi animals showed significant differences with CC control animals (A and B: one way ANOVA, Tukey post hoc test). C and D. The CI/PI animals exhibited short-term memory impairment evidenced as less time in the novel object compared to CI/PC animals at both time point studied (C) (unpaired *t* test between CC/PI and CI/PI; 2 way-ANOVA, Bonferroni post hoc test between all the CI/PI and CI/PC groups). The DI also demonstrated an impairment of working memory as shown by decreasing index in both studied time points (D) (unpaired *t* test between CC/PI and CI/PI; 2 way-ANOVA, Bonferroni post hoc test between all the CI/PI and CI/PC groups). E-G The anxiety-like symptoms were demonstrated in CI/PI animals by and increased faecal foli (E) (unpaired *t* test between CC/PI and CI/PI; 2 way-ANOVA, Bonferroni post hoc test between all the CI/PI and CI/PC groups), less rearing number (F) (unpaired *t* test between CC/PI and CI/PI; 2 way-ANOVA, Bonferroni post hoc test between all the CI/PI and CI/PC groups), and less time in the centre (G) (unpaired *t* test between CC/PI and CI/PI; 2 way-ANOVA, Bonferroni post hoc test between all the CI/PI and CI/PC groups). H The exploratory activity significantly decreases in CI/PI animals compared to CI/PC animals at both time points studied. (unpaired *t* test between CC/PI and CI/PI; 2 way- ANOVA, Bonferroni post hoc test between all the CI/PI and CI/PC groups). *n* = 10–12/group for behavioural test. ns $p \geq 0.05$, $^{*}p < 0.01–0.05$, $^{**}p < 0.001–0.01$, $^{***}p < 0.0001–0.001$, $^{****}p < 0.0001$.

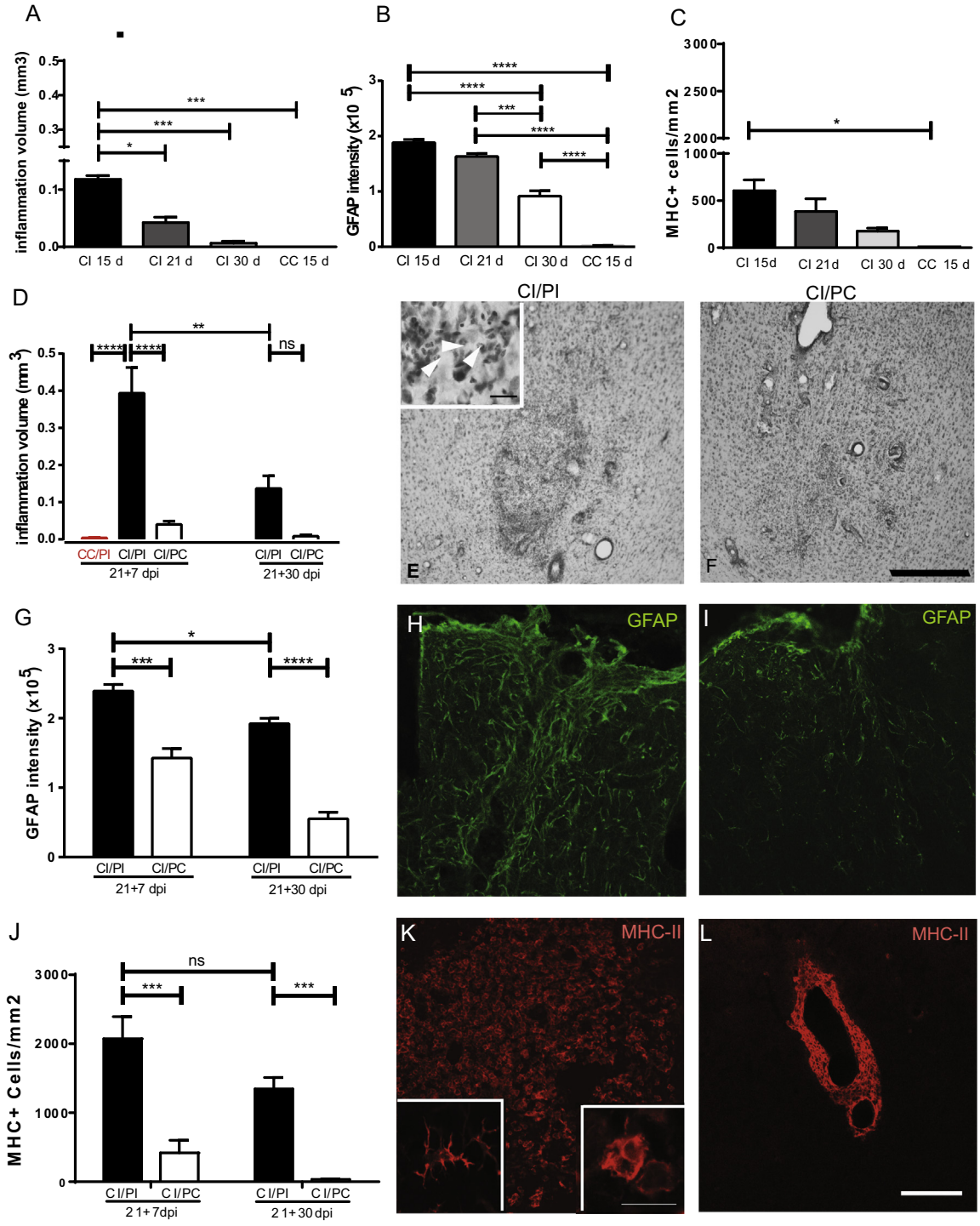

Fig. 3. Neuroinflammation and glial activation. (A–C) Analysis of the inflammation and glial activation in central injected animals with AdIL-1β or Adβgal (CI and CC, respectively). A. Quantification of the inflammatory volume at different time points after the injection. Significant differences were found between CI CC 15, 21 and 30 dpi and also between CI and CC 15 dpi (one way ANOVA, Tukey post hoc test.). B. Quantification of GFAP positive cells that demonstrate astroglia activation. Significant differences were found between CI 15, 21 and 30 dpi and also between CI and CC 15 dpi (one way ANOVA, Tukey post hoc test). C. Quantification of MHC-II positive cells that demonstrate microglia activation. Significant differences were found between CI 15 dpi and CC 15 dpi. (one way ANOVA, Tukey post hoc test). D–F. A sustained peripheral pro-inflammatory stimulus exacerbates central inflammation. D. Quantification of the inflammatory volume. Significant differences were found between CI/PI and CC/PI animals at 21 + 7 and 21 + 30 groups. (unpaired *t* test between CC/PI and CI/PI, 2 way-ANOVA and Bonferroni post hoc test between all the CI/PI and CI/PC groups). B and C. Representative low magnification pictures of the inflammatory lesions stained with Cresyl Violet. CI/PI 21 + 7 animals presented an important inflammatory infiltrate compared with CI/PC animals. Inset demonstrated a great amount of PMN neutrophils (arrows) in CI/PI animals compared with controls. G–I. Astroglia response to peripheral stimulation within central lesion. G. Quantification of GFAP intensity (2 way-ANOVA, Bonferroni post hoc test). H and I. Representative pictures of glial fibrillary acidic protein (GFAP) immunofluorescence. GFAP reactivity is increased in CI/PI 21 + 7 and 21 + 30 animals (H) compared with CI/PC animals (I). J–L. Microglia response to peripheral inflammatory stimulus within the central lesion. J. Quantification of MHC-II positive cells confirmed significant increase in the CI/PI 21 + 7 and 21 + 30 animals (2 way-ANOVA, Bonferroni post hoc test). K and L. Representative immunofluorescences against macrophage/microglia marker MHC-II. The CI/PI 21 + 7 and 21 + 30 groups had more MHC II + cells in the cortical parenchyma (K), than CI/PC group (L). Most of the MHC-II positive cells are type 3 (left inset) and Type 4 (right inset). E and F. Scale Bar: 200 μm, inset fig. E: 30 μm, H,I,K,L. Scale bar: 100 μm, Inset Fig. K: 20 μm. n = 8–10/group for histology. ns $p \geq 0.05$, $^{*}p < 0.01$–0.05, $^{**}p < 0.001$–0.01, $^{***}p$ 0.0001–0.001, $^{****}p < 0.0001$. (For interpretation of the references to colour in this figure legend, the reader is referred to the web version of this article.)

the microglia remained chronically activated for 50 days (Fig. 3K). In contrast, decreased astroglia activation was observed between the CI/PI 21 + 7 and CI/PI 21 + 30 animal groups, and significant differences in astroglia activation were found between the CI/PI and control groups (CI/PC) at 50 days, suggesting that the astroglia remained activated (Fig. 3G).

3.3. Chronic expression of IL-1β in the cortex induced demyelination

The central lesions exhibited demyelination with a pattern similar to that described for neuroinflammation. The demyelination volume peaked at 15 dpi and decreased up to 30 dpi (Fig. 4A). Additionally, at the ultrastructural level, some demyelinated axons

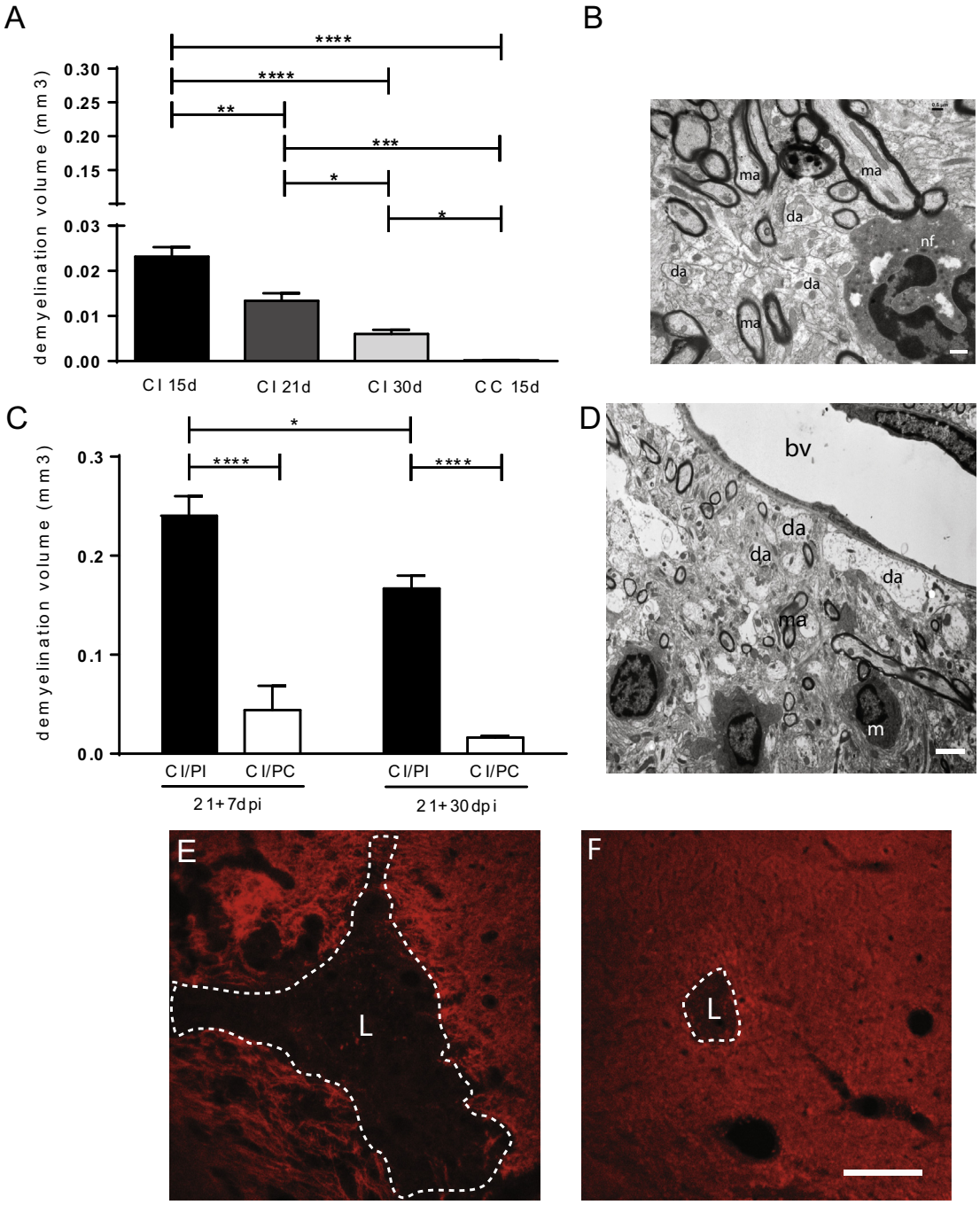

Fig. 4. Demyelination in cortical lesions. A. Quantification of the demyelination in CI animals at 15, 21 and 30 dpi and in CC animals 15 dpi (one way ANOVA, Tukey post hoc test) (staining Red Oil). B. Representative photomicrograph of the cortex of CI 21 dpi animals. Demyelinated axons (da) can be observed within the inflammatory region. Myelinated axons (ma) can also be observed widespread in the lesion. Nf: neutrophil. C–F. The peripheral stimulation induced demyelination. C. Quantification of the demyelination. The CI/PI 21 + 7 group had an extensive demyelination area compared with CI/PC 21 + 30 group (2 way-ANOVA, Bonferroni post hoc test). D. Representative photomicrograph of the cortex of CI/PI 21 + 7 animals. Demyelinated axons (da) can be observed within the inflammatory region. Myelinated axons (ma) can also be observed widespread in the lesion. m: microglia/macrophages, bv: blood vessel. E and F. Representative pictures of the demyelination in the cortex visualized by Myelin Binding Protein (MBP) staining. The CI/PI 21 + 7 animals exhibited an extended lesion area (L, dashed line) with MBP + axons surrounded the lesion (L, dashed line) compared with CI/PC 21 + 7 animals, which exhibited a smaller lesion (L, dashed line) area also surrounded by MBP + axons. B. Scale bar: 1 μm. D. Scale bar: 2 μm, Scale bar: 200 μm. E and F: Scale bar: 200 mm. n = 8–10/group for histology. $^{*}p < 0.01$–0.05, $^{**}p < 0.001$–0.01, $^{***}p < 0.0001$–0.001, $^{****}p < 0.0001$. (For interpretation of the references to colour in this figure legend, the reader is referred to the web version of this article.)

could be observed in CI/PI animals at 21 dpi (Fig. 4B). No demyelination was observed in CC animals (Fig. 4A).

The AdIL-1β-induced peripheral inflammation increased the demyelination volume in CI/PI animals compared with the CI/PC control group at both time points studied (21 + 7 and 21 + 30) (Fig. 4C). The demyelination was confirmed by myelin basic protein (MBP) immunofluorescence (Fig. 4E and F). At the ultrastructural level, demyelinated axons, intercalated with thinner myelinated axons, could be observed within the lesions. Additionally, myelinated axons were widespread throughout the lesions. Interestingly, in addition to the presence of neurodegenerative axons (see below), the neurofilaments and microtubules of the majority of axons were intact, further suggesting some preservation of axonal integrity (Fig. 4D).

3.4. Neurodegeneration and axonal damage can be observed in peripherally exacerbated cortical lesions

Peripheral exacerbation of cortical lesions induced neurodegeneration and axonal damage. To evaluate the presence of neurodegenerative neurons in the lesions, we assessed amyloid precursor protein-positive cells (APP+), fluoro-jade C (FJC)+ cells and NeuN/activated caspase 3+ cells (Fig. 5).

FJC was also used to analyse the presence of degenerative neurons. The FJC intensity was significantly increased in CI/PI animals compared with CI/PC animals at both time points (Fig. 5A–C), indicating enhanced neurodegeneration in the CI/PI group. The presence of APP+ cells demonstrated that degenerative axons were observed in the lesions (Fig. 5K and L). The APP+ degenerative axons were increased in CI/PI 21 + 7 animals, compared with CI/PC 21 + 7 animals (Fig. 5L). The APP + label was associated with both typical neuronal morphology, as well as varicose fibres and huge swelling, demonstrating the presence of degenerative axons (Fig. 5M).

We next evaluated the number of NeuN+ cells in the lesions. We found that the number of NeuN+ cells was significantly decreased in the AdIL-1β peripherally exacerbated animals, with a small number of healthy neurons observed in these animals (Suppl Fig. 3D–F). We also evaluated neuronal apoptosis using activated caspase 3. The CI/PI animals exhibited an increased number of NeuN+/Activated caspase 3+ cells compared with CI/PC control animals at both time points (Fig. 5D–J).

At the ultrastructural level, axonal degeneration was evidenced as swollen axons displaying abnormal-appearing organelles and electron-dense vesicles in CI/PI animals (Fig. 5M).

Taken together, these results indicated greater neurodegeneration and axonal damage in CI/PI rats compared with CI/PC rats.

Neurodegeneration in central lesions is demonstrated in Suppl. Fig. 3.

3.5. Presence of meningeal inflammation after central and peripheral inflammation

The presence of meningeal inflammation and B-cell follicle-like structures characteristic of SPMS is mostly associated with cortical pathology in MS patients (Magliozzi et al., 2007; Serafini et al., 2004). Thus, we evaluated the presence of meningeal inflammation in the experimental animals.

The animals with chronic IL-1β-induced lesions (CI) and peripherally stimulated animals (CI/PI) exhibited meningeal inflammation characterized by an inflammatory infiltrate mostly composed of macrophages, lymphocytes, neutrophils, and follicular dendritic cells (Fig. 6). Additionally, cuffed vasodilated blood vessels were also observed in the subarachnoid space (Fig. 6A). These vasodilated vessels, which were surrounded by inflammatory infiltrate, resembled the follicle-like structures present in human PPMS and SPMS patients (Howell et al., 2011; Magliozzi et al., 2007). The follicle-like structures were surrounded by a complex reticular network of collagen type IV fibrils, along with neutrophils, macrophages, and lymphocytes. To further characterize the lymphocyte composition of these follicle-like structures, we used a panel of antibodies described as key features of these structures. We found CD4+, CD8+, CD45RC+, CD39+, and CD20+ cells in the meninges. Follicular dendritic cells were observed as CD23+ cells in the meninges of CI/PI animals (Fig. 6B–G). When comparing the number of these vasodilated vessels surrounded by the inflammatory infiltrate, CI/PI animals (both 21 + 7 and 21 + 30) showed no statistically significant differences between these two groups (21 + 7 and 21 + 30) (Fig. 6H).

The presence of follicle-like structures has been correlated with microglial activation and grey matter inflammation in progressive MS patients (Howell et al., 2011). We evaluated whether correlations existed among these features to determine whether an association among these parameters was present in our model. Interestingly, we found that CI/PI 21 + 7 animals that received pro-inflammatory peripheral stimulation exhibited a strong, positive correlation between the meningeal inflammation, described as the number of cuffed dilated blood vessels and inflammation. Statistically significant correlations between the numbers of these structures and microglial activation, astroglial activation, and neurodegeneration were also observed at both time points studied (21 + 7 and 21 + 30). (Fig. 6I–N)

The correlation between the number of these structures and the inflammatory volume at 21 + 7 was robust (Suppl Fig. 4C). However, no positive correlation was found at 21 + 30 dpi (Suppl Fig. 4D), perhaps because of the decreased inflammatory volume in the CI/PI 21 + 30 animals, compared with the CI/PI 21 + 7 group (Fig. 3D).

3.6. The in vivo evolution of peripherally stimulated cortical lesions can be observed using MRI imaging

We performed several MRI sequences to follow the *in vivo* evolution of the cortical lesions at different time points following central injections of either AdIL-1β or Adβgal. The non-peripherally stimulated cortical lesions induced by the long-term expression of IL-1β in the cortex could not be observed in the brain on MRI in any of the performed sequences (data not shown). Interestingly, the peripherally stimulated cortical lesions of CI/PI 21 + 7 experimental animals could be visualized in the T2-weighted sequence (Fig. 7A), and they showed homogeneous enhancement of cortical lesion images with gadolinium in T1, with maximum enhancement at six minutes after gadolinium injection (Fig. 7D). These cortical lesions exhibited an extended inflammatory area (see Fig. 3), along with extensive BBB disruption (Fig. 7E). Cortical lesions were not observed on the MRI images of CI/PC 21 + 7 animals (Fig. 7F–I), although the BBB was open, and tissue damage was still present in control animals at this time point (Fig. 7J)

We did not observe cortical lesions on the MRI images of CI/PI 21 + 30 animals (data not shown), although neuroinflammation was present in the cortical tissue of the experimental animals. In contrast to the results obtained for CI/PI 21 + 7 animals, the BBB was restored at this time point.

3.7. Long-term expression of IL-1β in the cortex induced expression of pro-inflammatory cytokines

Upregulation of pro-inflammatory cytokines, such as IL-1β, IL-6, and TNF-α, has been observed in the plasma, lesions, and CSF of both MS animal experimental models and MS patients (Borjini et al., 2016; Murta et al., 2015; Pare et al., 2016; Seppi et al.,

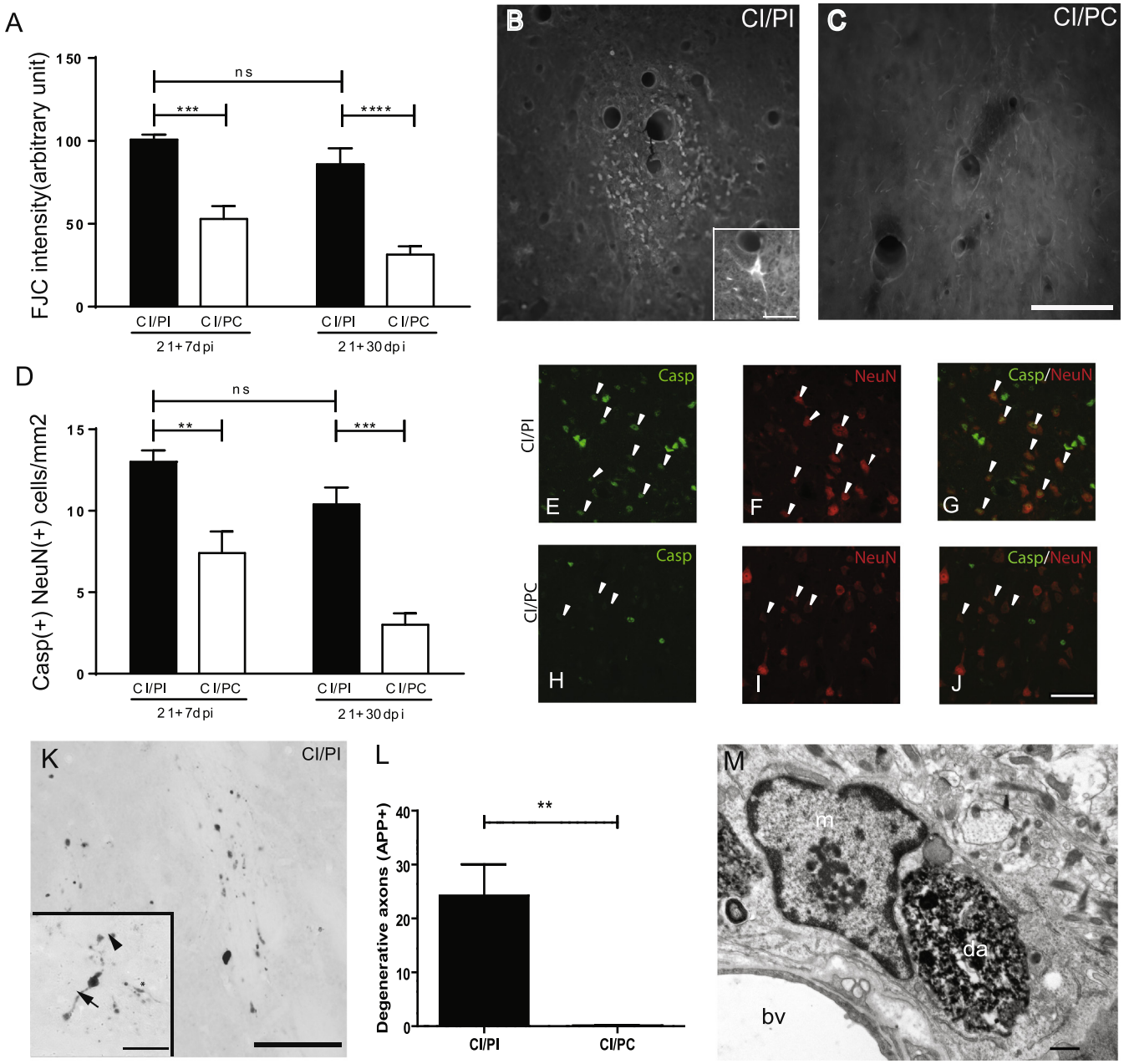

Fig. 5. Neurodegeneration and axonal damage can be observed in peripherally exacerbated cortical lesions. A-C- Neurodegeneration demonstrated by Fluorojade C (FJC) staining. A. Quantification of FJC intensity demonstrated significant differences between CI/PI and CI/PC at 21 + 7 and 21 + 30 groups (2 way- ANOVA, Bonferroni post hoc test). Representative pictures of the FJC staining of CI/PI (B) and CI/PC (C) 21 + 7 group. Inset: picture of a neurodegenerative cortical neuron stained with FJC. D. Quantification of NeuN+/Caspase 3 activated + cells (D) (2 way-ANOVA, Bonferroni post hoc test). CI/PI animals exhibited an increased number of NeuN+/Caspase 3 + compared to CI/PC control animals at both studied time points (D). E–J. Representative pictures of single and double staining NeuN/Caspase 3 in CI/PI 21 + 7 animals (E–G) and CI/PC 21 + 7 animals (H–J). K and L. Representative pictures of Amyloid Precursor Protein (APP) positive axons and neurons. CI/PI 21 + 7 animals showed APP positive axons. Inset: The APP positive axon showed the typical morphology with spheroid end bulb morphology (black arrowhead), small swellings (*), and varicose fibers (black arrows) in CI/PI 21 + 7 animals. L. APP-positive degenerative axons were statistically increased in CI/PI compared with CI/PC (Unpaired *t* test). M. Representative photomicrograph of a microglia (m) that phagocyted a degenerative axon (da) with electron dense vesicles within its axolema as observed in CI/PI 21 + 7 animals. B, C, K. Scale bar: 100 μm. Inset fig. K Scale bar: 50 μm, E–J. Scale bar: 50 μm, M. Scale bar: 1 μm. $n = 8–10$/group for histology. $n = 4$/group for APP. ns $p \geq 0.05$, $^{**}p$ 0.001–0.01, $^{***}p < 0.0001–0.001$, $^{****}p < 0.0001$. (For interpretation of the references to colour in this figure legend, the reader is referred to the web version of this article.)

2014). Therefore, we examined whether these pro-inflammatory cytokines were also upregulated in IL-1β-induced lesions.

CI-injected animals exhibited maximum expression of TNF-α at CI 21 dpi, with significant differences between CI 15 dpi and CI 30 dpi. However, at 30 dpi, the expression of TNF-α was still significantly increased, compared with CC 15 dpi animals (Fig. 8A). IL-6 expression peaked at 21 dpi with significant differences at CI 21 dpi, compared with the CI 15 and 30 dpi groups (Fig. 8C). CC 15 dpi animals displayed very small amounts of any of the analysed pro-inflammatory cytokines (Fig. 8A–C).

Peripheral stimulation increased pro-inflammatory cytokine mRNA expression in the chronic central cortical lesions. The CI/PI 21 + 7 and 21 + 30 groups showed increased expression of TNF-α and IL-6 in the ipsilateral cortex (Fig. 8B and D). The expression of both cytokines was sustained for almost 50 days, demonstrating the chronicity of the inflammatory event. This upregulation was

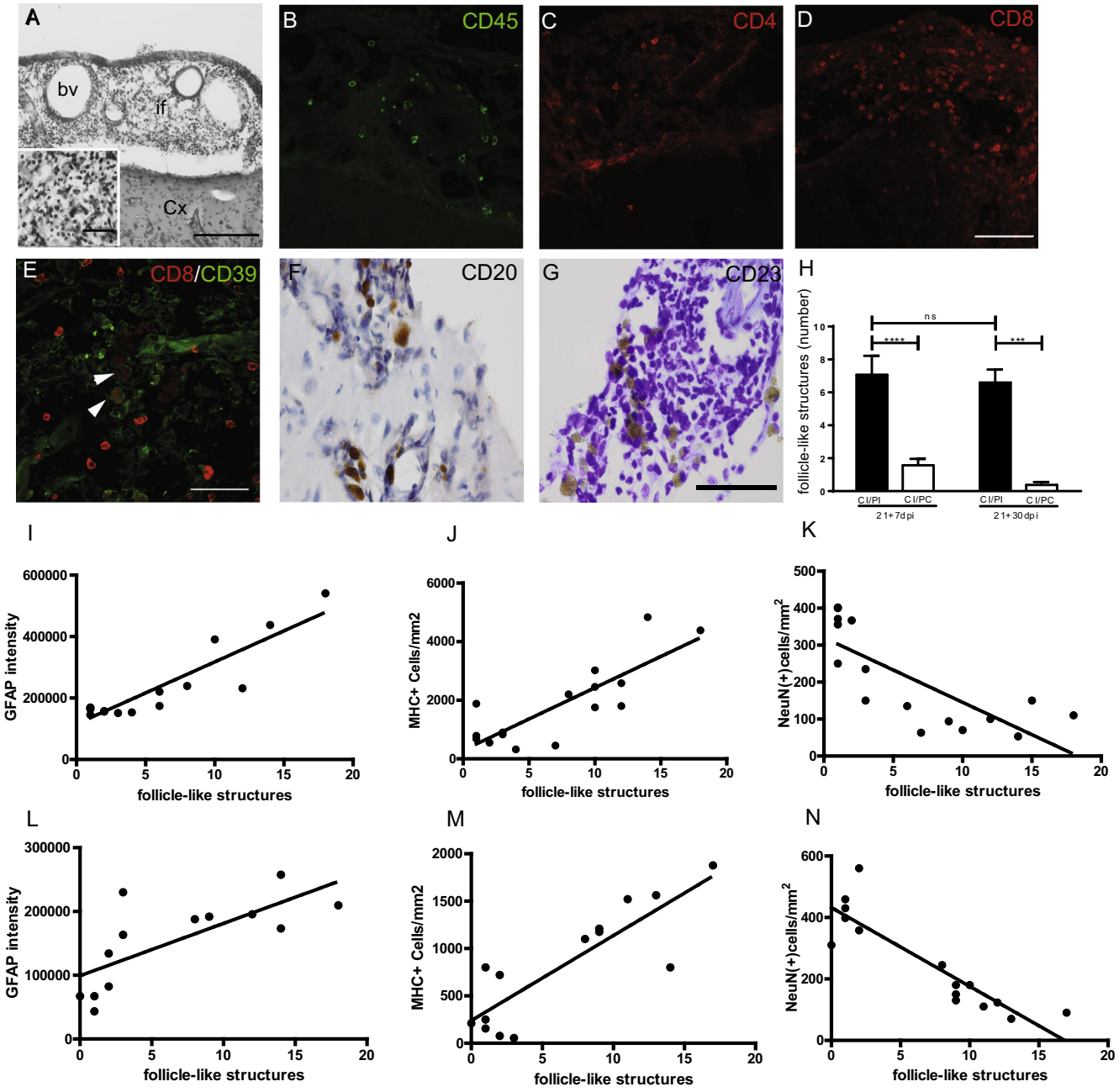

Fig. 6. Peripheral stimulated cortical lesions induce meningeal inflammation. A. Representative picture of inflammation in the meninges was observed with inflammatory infiltrated within the meninges and cuffed vasodilated blood vessels in CI/PI 21 + 7animals. The inset demonstrated the inflammatory infiltrate in the meningeal inflammation. Staining: Cresyl violet. B–F. T and B cells were observed as CD45RC+, CD4+, CD8+, CD39+ and CD20+ cells. Follicular dendritic cells we observed as CD23+ cells (G) in the meninges. H. Quantification of the number of cuffed blood vessel in the meninges demonstrated an increased number in CI/PI compared to CI/PC animals at both time points studied. Statistical analysis was performed with 2 way-ANOVA and Bonferroni post hoc test. ns $p \geq 0.05$, $^{***}p < 0.0001$–0.001, $^{****}p < 0.0001$. I and K. Correlations between astroglia intensity (Spearman test, r = 0.73, $p = 0.0012$, $r^2 = 0.81$) (I), microglia activation (Spearman test, r = 0.70, p = 0.0022, $r^2 = 0.67$) (J) and NeuN density (Spearman test, r = −0.80, $p = 0.0002$, $r^2 = 0.59$) (K) in CI/PI 21 + 7 animals. L–N. Correlations between astroglia intensity (Spearman test, r = 0.82, $p = 0.0005$, $r^2 = 0.53$) (L), microglia activation (Spearman test, r = 0.73, $p = 0.0025$, $r^2 = 0.72$) (M) and NeuN + density (Spearman test, r = −0.88, $p = <0.0001$, $r^2 = 0.79$) (N) in CI/PI 21 + 30 animals. Cx: cortex, bv: blood vessel, if: inflammatory infiltrate. A. Scale bar: 200 μm, Inset: 50 μm. B–E Scale bar: 50 μm, F and G. Scale bar: 100 μm. $n = 8$–10/group for histology. (For interpretation of the references to colour in this figure legend, the reader is referred to the web version of this article.)

significant when comparing CI/PI and CI/PC animals. Interestingly, the increase in these cytokines was almost ten-fold, compared to the expression of the same cytokines in CI non-stimulated animals (Fig. 8B and D).

4. Discussion

We developed a simple animal model that represents most of the characteristics of the cortical involvement in progressive forms of MS, such as cognitive impairment associated with cortical neuroinflammation, demyelination, neurodegeneration, and meningeal inflammation, which were exacerbated by peripheral stimulation and could be visualized by MRI. The peripheral stimulation allowed for the maintenance of the chronicity of cortical lesions, which lasted for 50 days. The cortical pathology reflects the progression of disabilities and demonstrates that this pathology plays a role in disease progression. Progressive forms of MS are characterized by a gradual progression of clinical disabilities,

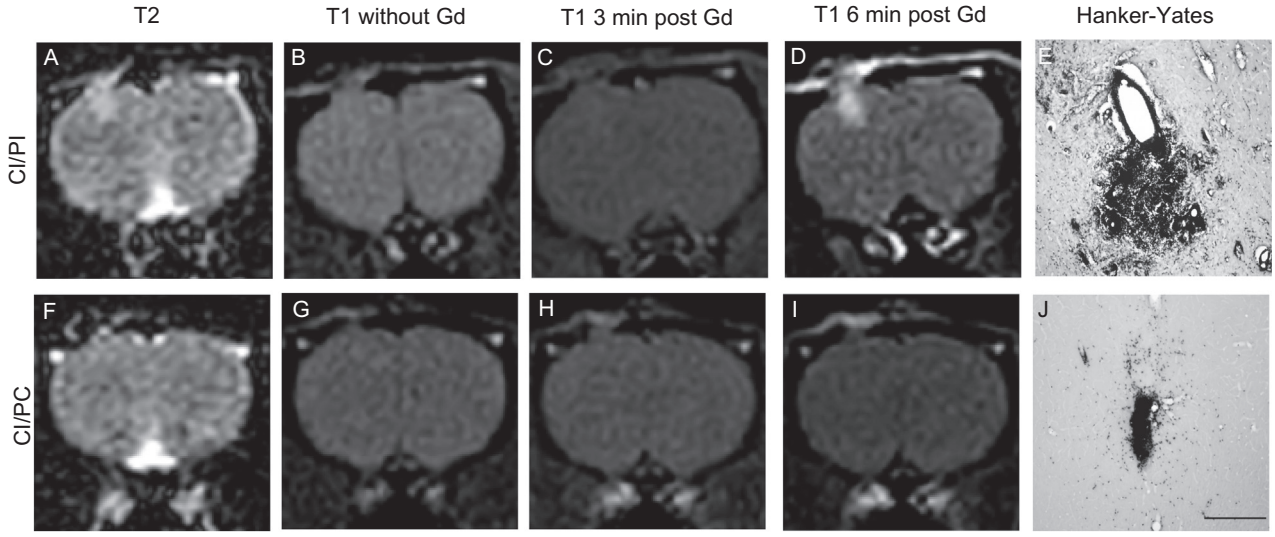

Fig. 7. MRI sequences in order to follow the *in vivo* evolution of the cortical lesions. The peripherally stimulated cortical lesions of CI/PI 21 + 7 experimental animals can be visualized in T2-weighted sequence (A–D), with maximum enhancement six minutes after the gadolinium injection (D). These cortical lesions exhibited an extensive BBB disruption as observed with the Hanker-Yates technique (E). The MRI images of the cortical lesions could not be observed in CI/PC 21 + 7 animals (F–I), even though that the BBB was opened (J). E–J. Scale bar: 200 μm. n = 4/group for MRI.

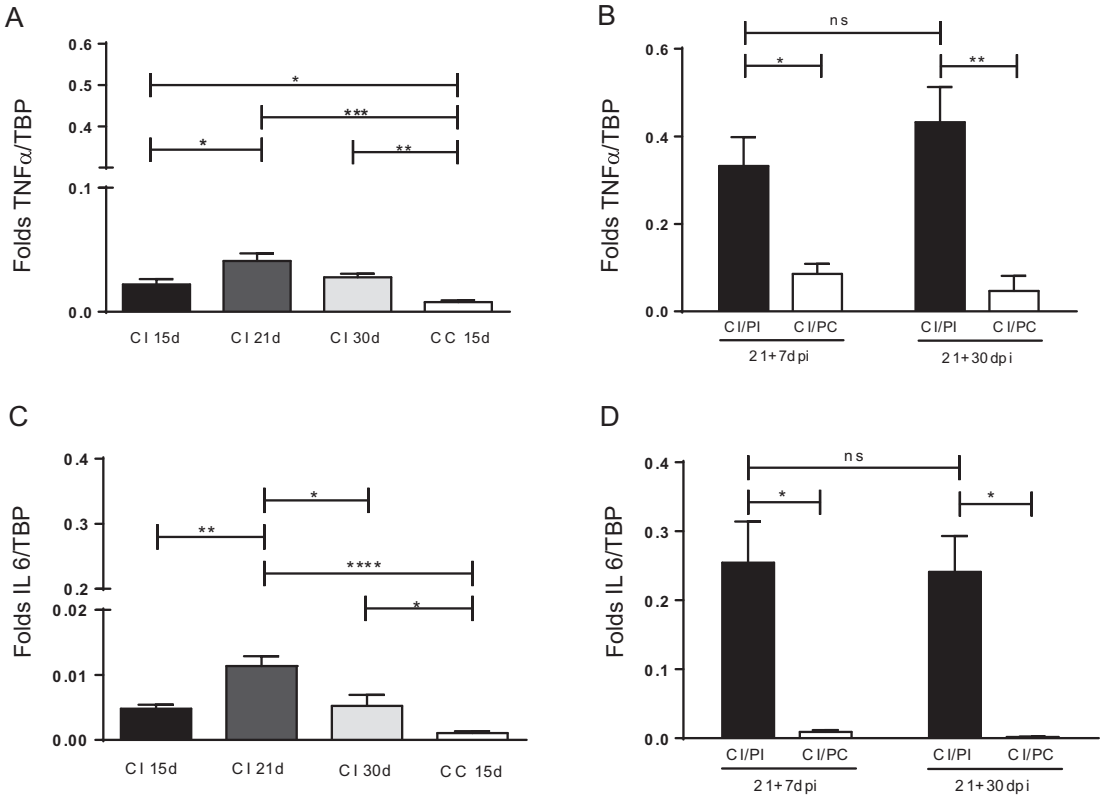

Fig. 8. Both central and peripherally stimulated sustained inflammatory stimulus upregulates central cytokine expression. A and C. Central injection of IL-1β in the cortex induced TNF-α (A) and IL-6 expression (C) (one way ANOVA, Tukey post hoc test) had a maximum at 21 dpi. B and D. The peripherally stimulated animals showed an increased pro-inflammatory cytokines expression in CI/PI animals compared to CI/PC animals at 21 + 7 and 21 + 30 The peripherally stimulated lesions showed an increased TNF-α (B) and IL-6 expression (D) (2 way-ANOVA, Bonferroni post hoc test) in CI/PI animals compared to CI/PC animals at 21 + 7 and 21 + 30 (e). n = 5–6/group for real-time PCR. ns $p \geq 0.05$, $^{*}p < 0.01$–0.05, $^{**}p < 0.001$–0.01, $^{***}p$ 0.0001–0.001, $^{****}p < 0.0001$. TBP: TATA box binding protein.

along with cortical lesions and meningeal inflammation. Although these signs can be observed in RRMS, they are less frequent (Howell et al., 2011; Magliozzi et al., 2007; Serafini et al., 2004). It is important to emphasize that there is no therapeutic treatment for SPMS, and affected patients experience continual worsening of symptoms. However, there is currently only one treatment for PPMS (Frampton, 2017). Several animal models have been reported to represent the progressive forms of MS, but these models have not reflected the chronicity and pathophysiology of the progressive lesions (Pryce et al., 2005).

In this study, cortical lesions were induced with an IL-1β-expressing adenovirus to achieve long-term cytokine expression

(Ferrari et al., 2004; Murta et al., 2012, 2015). IL-1β has been strongly associated with MS pathology in both humans and animal models (Borjini et al., 2016; Brosnan et al., 1995; Dujmovic et al., 2009; Hauser et al., 1990; Herges et al., 2012; Levesque et al., 2016; Liu et al., 2010; Naegele et al., 2011; Pare et al., 2016; Pelletier et al., 2010; Tsukada et al., 1991; Wu et al., 2010). Few rodent EAE models have shown cortical pathology (Gardner et al., 2013; Lagumersindez-Denis et al., 2017; Mangiardi et al., 2011; Merkler et al., 2006; Stassart et al., 2015; Ucal et al., 2017). However, these models partially represent the features observed in the cortices of progressive MS patients. Additionally, systemic inflammation exacerbates chronic central lesions. The phenomenon of a systemic stimulus flare-up of the symptoms of neurodegenerative diseases has been described in previous studies, both in humans and in animal models (Buljevac et al., 2002; Cunningham et al., 2005; Holmes et al., 2009; Moreno et al., 2011; Murta et al., 2015; Pott Godoy et al., 2010; Teeling and Perry, 2009).

Long-term expression of IL-1β impaired short-term memory in our model. Peripheral stimulation exacerbated memory deterioration, demonstrating that the cognitive changes were chronic. These features resembled the clinical situation. MS patients suffer from chronic cognitive impairment with short-term memory problems, inducing considerable deterioration in quality of life. Currently, no specific treatments for these impairments have been developed (Amato et al., 2008; Brissart et al., 2012). In accordance with our results, cognitive impairment could also be affected by systemic inflammation in MS patients; indeed, its exacerbation has been described in the peripheral inflammatory context during the relapse phase (Benedict et al., 2014; Foong et al., 1998; Morrow et al., 2011). Additionally, pro-inflammatory systemic stimuli induced anxiety-like behaviour in animals already presenting with central lesions. In our study, the peripherally stimulated animals spent less time in the light area and showed fewer rears and more faecal boli. IL-1β has been described as inducing decreased locomotor activity and anxiety-like behaviour in rodents (Chen et al., 2008; Dunn et al., 2006; Swiergiel and Dunn, 2007). Indeed, it has been shown to be involved in anxiety-like behaviour in EAE (Gentile et al., 2016). However, IL-1β also induces "sickness behaviour" (Dantzer et al., 1991; Dantzer et al., 1998; Shimommura et al., 1990), suggesting that the anxiety-like symptoms are due to a reduction in the general activity of the animals (Swiergiel and Dunn, 2007), providing an alternative explanation for our results. Accordingly, high prevalence of anxiety symptoms has been reported in MS patients (Butler et al., 2016; Litster et al., 2016). Interestingly, several studies have shown a significant correlation of cognitive dysfunction with increased anxiety (Butler et al., 2016). Indeed, the prefrontal cortex has been described to be involved in short-term memory and recognition memory circuits (Erickson et al., 2010; Fuster and Alexander, 1971; Larocque et al., 2014; Morici et al., 2015), as well as in the regulation of stress and anxiety (Charney, 2003; Kjaerby et al., 2016).

In our model, the long-term expression of IL-1β in the cortex induced neuroinflammation with immune cell recruitment, including of neutrophils and microglia/macrophages, as well as BBB breakdown and astroglial and microglial activation. These features have been described in MS pathology and in most MS animal models. IL-1β and PMNs have been strongly associated with MS human pathology and MS animal experimental models (Borjini et al., 2016; Brosnan et al., 1995; Burm et al., 2016; Dujmovic et al., 2009; Hauser et al., 1990; Herges et al., 2012; Liu et al., 2010; Naegele et al., 2011; Pare et al., 2016; Pelletier et al., 2010; Tsukada et al., 1991; Wu et al., 2010). The presence of cortical neuroinflammation has been described in early-stage MS patients. Chronic cortical lesions exhibit less inflammation than white matter lesions, with neither inflammatory lymphocytes nor macrophages in MS patients (Lucchinetti et al., 2011; Popescu and Lucchinetti, 2012). The EAE model has contributed to the study of MS pathophysiology and the development of therapeutic agents, but the scarcity of EAE analyses of cortical lesions in this model has led to some limitations in studying the cortical pathology and progressive forms of MS. To develop a model for the progressive forms, a variant of chronic EAE was induced in C57BL/6J mice, in which the disease did not remit. This model is very useful for studying the function of CD8, CD4, B cells and monocytes during the pathogenesis of the disease. As a limitation, areas of demyelinated axons do not occur in predictable locations; therefore, their use for the study of the mechanism of local demyelination is limited (Ransohoff, 2006). Chronic relapsing EAE in the Biozzi antibody high (ABH) mouse develops key features of secondary progressive disease with progressive disability, demyelination, axonal damage, neurodegeneration, and gliosis but with no cortical lesions (Hampton et al., 2008; Pryce et al., 2005). The presence of cortical lesions has also been described in EAE in marmosets, mice, Lewis rats immunized with a cocktail of cytokines, and animals with EAE stereotactically injected with TNF-α in the cortex and in a modified cuprizone model (Bai et al., 2016; Gardner et al., 2013; Merkler et al., 2006; Stassart et al., 2015).

The IL-1β-induced cortical lesions exhibited neurodegeneration and axonal damage in our model. Importantly, neurodegeneration has been described in progressive human MS cortical lesions, which could be responsible for the cognitive impairment and worsening of disease outcomes in MS patients (Calabrese et al., 2012, 2013; Lucchinetti et al., 2011; Nelson et al., 2011). Indeed, grey matter damage is a better predictor of physical disability and cognitive impairment than white matter damage (Zivadinov and Pirko, 2012). Furthermore, axonal damage correlates with inflammation in both MS and EAE (Dutta and Trapp, 2011; Mangiardi et al., 2011). Finally, IL-1β causes excitotoxic neurodegeneration and synaptic hypersensitivity in MS patients (Rossi et al., 2012, 2014), highlighting the relevance of neurodegeneration in this disease.

We found that meningeal inflammation was associated with IL-1β-induced cortical lesions mostly in CI/PI animals. It is important to emphasize that no meningeal inflammation has been reported when AdIL-1β is injected either into the striatum or into the substantia nigra (Murta et al., 2012, 2015; Pott Godoy et al., 2010). The clinical setting was again modelled in CI/PI animals: meningeal inflammation and follicle-like structures have been primarily described in SPMS and PPMS patients and in animal models (Choi et al., 2012; Christy et al., 2013; Howell et al., 2011; Magliozzi et al., 2004, 2007; Serafini et al., 2004). In patients with progressive MS forms, compartimentalized diffuse meningeal inflammation has been associated with increased cortical demyelination, neurodegeneration, glial activation, and a more severe disease outcome (Choi et al., 2012; Howell et al., 2011; Mainero and Louapre, 2015). In accordance with our results, the presence of neutrophils in the meninges has also been described in meningeal inflammation in an EAE model (Christy et al., 2013). Interestingly, meningeal inflammation showed positive correlations with cortical neurodegeneration, glial activation, and demyelination at all of the analysed time points in our model. However, the correlation between meningeal inflammation and the volume of cortical inflammation was only observed at early time points, at which inflammation was more evident. Increased cortical demyelination, neurite loss and more severe clinical outcomes have been associated with greater meningeal inflammation in PPMS patients (Choi et al., 2012). Additionally, the presence of B cell follicle-like structures and increased meningeal inflammation was positively correlated with microglial activation and cortical grey matter demyelination in SPMS patients (Howell et al., 2011). Most studies have described meningeal inflammation as a previous step in the

development of cortical damage in MS. However, in our model, we first induced cortical lesions and then observed diffuse meningeal inflammation. Therefore, meningeal inflammation should be considered a key factor in cortical lesions, although its role in cortical pathology should be addressed due to the lack of knowledge regarding whether meningeal inflammation induces cortical lesions or vice versa.

Different studies in animal models have shown that cortical lesions can be visualized *in vivo* using structural and functional MRI (Serres et al., 2013; Stassart et al., 2015; Tambalo et al., 2015). In our study, only the peripherally stimulated central lesions CI/PI 21 + 7 could be demonstrated *in vivo* using MRI in T2-weighted and T1-weighted gadolinium enhancement sequences. At this time point, the exacerbated lesions exhibited maximum neuroinflammation and BBB disruption. Although tissue damage and BBB leakage were present at 15, 21, and 30 dpi and 21 + 7 and 21 + 30 CI/PC, they were not observed with MRI under any condition, resembling the phenomenon described as normal-appearing grey matter (NAGM) (Calabrese and Castellaro, 2017; Klaver et al., 2015). In addition, gadolinium enhancement of T1-weighted lesions reflects BBB rupture during the inflammatory phase of the disease. This gadolinium enhancement is less frequent on MRI with the progressive forms of MS. BBB leakage in chronic lesions cannot be visualized by conventional MRI. The use of conventional MRI protocols to demonstrate BBB leakage in MS patients has been the subject of discussion (Filippi et al., 1995; Silver et al., 2001).

The cortical lesions induced by IL-1β revealed upregulation of the mRNA of pro-inflammatory cytokines, including IL-1β, IL-6, and TNF-α, in our model. The upregulation of IL-1β, IL-6, and TNF-α has been observed in serum, plasma, lesions, and CSF in both EAE models and MS patients (Borjini et al., 2016; Kallaur et al., 2016; Pare et al., 2016; Valentin-Torres et al., 2016). Indeed, IL-1β and TNF-α play roles both in neurodegeneration and as neurotoxic molecules in PMS, respectively (Kempuraj et al., 2016; Rossi et al., 2014). It is important to highlight that in our model, we observed higher levels of TNF-α and found neurodegeneration in cortical lesions. It will be interesting to perform additional studies to elucidate whether there is a direct effect of TNF-α on neurodegeneration. Additionally, elevated expression levels of IL-1β and TNF-α are likely indicative of the initiation of BBB breakdown (Borjini et al., 2016). In our model, BBB damage was evident in cortical lesions induced by chronic expression of IL-1β, as described previously. However, even when the BBB was restored, neuroinflammation was evident in these lesions (data not shown). These results agreed with findings demonstrating that, in the progressive forms, inflammation remains enclosed behind an intact BBB (Bradl and Lassmann, 2009).

In summary, we developed an experimental model mimicking the cortical damage in the progressive forms of MS with several relevant similarities to the clinical setting and based on the peripheral stimulation of an ongoing pro-inflammatory central lesion. Indeed, our model offers chronic cortical lesions with demyelination, neurodegeneration and neuroinflammation, along with cognitive deficiencies similar to those observed in the human pathology. Additionally, both pathological features and cognitive impairment can be boosted by peripheral injection of pro-inflammatory cytokines, resembling the chronicity of human lesions. All of these pathological features were triggered by the long-term expression of a unique pro-inflammatory cytokine, allowing for the study of the role of the innate immune system in the pathology of MS. Compared to other models of cortical damage (see Table 1), our model is based on innate immunity, and it reflects the chronicity, demyelination, neurodegeneration, cognitive impairment, and anxiety-like symptoms that characterize MS cortical lesions. Additionally, these lesions can be visualized using MRI. The findings described using this new model might have implications for studying and understanding some pathological aspects of the progressive forms of MS, especially those related to cortical lesions and worse clinical outcomes.

5. Conclusion

We developed a chronic inflammatory focal cortical model triggered by the innate immune system, which exhibits most of the hallmarks of the cortical pathology of the progressive forms of MS, such as neuroinflammation, demyelination, glial activation, and neurodegeneration, along with cognitive symptoms. We also demonstrated the presence of meningeal inflammation, which was very similar to that described in MS patients. Additionally, we described a flare-up of the cortical lesions after peripheral inflammation, demonstrating the influence of systemic inflammation on central lesions.

The proposed model exhibited very important features, compared with other cortical models.

- Regarding behavioural symptoms, this model is the only one to demonstrate short-term memory impairment, which is among the main symptoms in MS patients. This symptom could be useful for the development of therapeutic strategies for this issue.
- At the pathological level, this model could enable studies of the functional roles of the innate immune system, glia and BBB in disease progression. Additionally, because we have described meningeal inflammation, the model could help to elucidate the mechanisms underlying the interaction between the cortex and meninges and additionally could be useful for identifying molecular biomarkers in the CSF. Furthermore, peripheral exacerbation will allow for examination of the effect of peripheral inflammation on central cortical lesions.
- IL-1β-exacerbated lesions were visualized by MRI. This model is one of the few in which lesions can be visualized using MRI, which could contribute to the development of technical methods for visualization of these lesions, such as the time of acquisition, the development of new contrast agents and new sequences for the visualization and specificity of cortical lesions. Additionally, we were able to reproduce the phenomenon of apparent normal grey mater, which could facilitate the development of specific techniques for the visualization of cortical lesions.

In summary, this model could enable the assessment of drugs in cortical damage scenarios, studies of the mechanisms underlying this damage and elucidation of meninges-cortex interactions. In addition, it could help to clarify the mechanisms involved in the interactions between cortical injuries and the peripheral pro-inflammatory environment. Considering that after almost 50 years of research in MS, a treatment for PPMS has only recently become available, and to date, there is no treatment for SPMS, the development of animal models for progressive MS would represent a milestone for the development and testing of new therapeutic agents and to improve our knowledge of the pathophysiology of progressive MS lesions.

Acknowledgments

CCF, FJP and MCL are members of the Research Career of the National Council of Scientific and Technological Research (CONICET), Argentina. MIF is a technician for CONICET. BAS is a fellow of the René Baron Foundation. BAS received a Fiorini Foundation award. We are grateful to Dr. Hernan García Rivello (Italian Hospi-

tal) for his assistance with the CD20 and CD23 immunohistochemistry. We thank Dr. Eduardo Castaño for his critical reading of the manuscript. We would also like to thank to Lucas D. Costa for his kind assistance in the statistical analysis (Unidad de Bioestadística aplicada a Ciencias de la Salud. Facultad de Ciencias Médicas. Universidad Nacional Del Litoral).

Sources of support

This work was supported by the National Council of Scientific and Technological Research (CONICET), Argentina, PIP grant 11220080100106 (CCF); by the National Agency for Scientific and Technological Promotion (ANPCyT), Argentina, PICT-2012-0656 grant (CCF); and by the René Baron Foundation.

Appendix A. Supplementary data

Supplementary data associated with this article can be found, in the online version, at https://doi.org/10.1016/j.bbi.2018.01.010.

References

Amato, M.P., Zipoli, V., Portaccio, E., 2008. Cognitive changes in multiple sclerosis. Expert Rev. Neurother. 8, 1585–1596.
Antunes, M., Biala, G., 2012. The novel object recognition memory: neurobiology, test procedure, and its modifications. Cogn. Process. 13, 93–110.
Argaw, A.T. et al., 2006. IL-1beta regulates blood-brain barrier permeability via reactivation of the hypoxia-angiogenesis program. J. Immunol. 177, 5574–5584.
Ascherio, A., Munger, K.L., 2016. Epidemiology of Multiple Sclerosis: from risk factors to prevention-an update. Semin. Neurol. 36, 103–114.
Bai, C.B. et al., 2016. A mouse model for testing remyelinating therapies. Exp. Neurol. 283, 330–340.
Benedict, R.H. et al., 2014. Characterizing cognitive function during relapse in multiple sclerosis. Mult. Scler. 20, 1745–1752.
Borjini, N. et al., 2016. Cytokine and chemokine alterations in tissue, CSF, and plasma in early presymptomatic phase of experimental allergic encephalomyelitis (EAE), in a rat model of multiple sclerosis. J. Neuroinflamm. 13, 291.
Bradl, M., Lassmann, H., 2009. Progressive multiple sclerosis. Semin. Immunopathol. 31, 455–465.
Brissart, H. et al., 2012. Working memory in multiple sclerosis: a review. Rev. Neurol (Paris). 168, 15–27.
Brosnan, C.F. et al., 1995. Cytokine localization in multiple sclerosis lesions: correlation with adhesion molecule expression and reactive nitrogen species. Neurology 45, S16–S21.
Buljevac, D. et al., 2002. Prospective study on the relationship between infections and multiple sclerosis exacerbations. Brain 125, 952–960.
Burm, S.M. et al., 2016. Expression of IL-1beta in rhesus EAE and MS lesions is mainly induced in the CNS itself. J. Neuroinflamm. 13, 138.
Butler, E., Matcham, F., Chalder, T., 2016. A systematic review of anxiety amongst people with Multiple Sclerosis. Mult. Scler. Relat. Dis. 10, 145–168.
Calabrese, M. et al., 2012. Cortical lesion load associates with progression of disability in multiple sclerosis. Brain 135, 2952–2961.
Calabrese, M. et al., 2013. Grey matter lesions in MS: from histology to clinical implications. Prion 7, 20–27.
Calabrese, M., Castellaro, M., 2017. Cortical gray matter MR imaging in multiple sclerosis. Neuroimag. Clin. N Am. 27, 301–312.
Cikos, S., Bukovska, A., Koppel, J., 2007. Relative quantification of mRNA: comparison of methods currently used for real-time PCR data analysis. BMC Mol. Biol. 8, 113.
Cunningham, C. et al., 2005. Central and systemic endotoxin challenges exacerbate the local inflammatory response and increase neuronal death during chronic neurodegeneration. J. Neurosci. 25, 9275–9284.
Charney, D.S., 2003. Neuroanatomical circuits modulating fear and anxiety behaviors. Acta Psychiatr. Scand Suppl., 38–50
Chen, J. et al., 2008. Neuroinflammation and disruption in working memory in aged mice after acute stimulation of the peripheral innate immune system. Brain Behav. Immun. 22, 301–311.
Choi, S.R. et al., 2012. Meningeal inflammation plays a role in the pathology of primary progressive multiple sclerosis. Brain 135, 2925–2937.
Christy, A.L. et al., 2013. Mast cell activation and neutrophil recruitment promotes early and robust inflammation in the meninges in EAE. J. Autoimmun. 42, 50–61.
Dantzer, R., Bluthe, R.M., Kelley, K.W., 1991. Androgen-dependent vasopressinergic neurotransmission attenuates interleukin-1-induced sickness behavior. Brain Res. 557, 115–120.
Dantzer, R. et al., 1998. Cytokines and sickness behavior. Ann. N Y Acad. Sci. 840, 586–590.
Denic, A. et al., 2011. The relevance of animal models in multiple sclerosis research. Pathophysiology 18, 21–29.
Dujmovic, I. et al., 2009. The analysis of IL-1 beta and its naturally occurring inhibitors in multiple sclerosis: the elevation of IL-1 receptor antagonist and IL-1 receptor type II after steroid therapy. J. Neuroimmunol. 207, 101–106.
Dunn, A.J. et al., 2006. Reduced ingestion of sweetened milk induced by interleukin-1 and lipopolysaccharide is associated with induction of cyclooxygenase-2 in brain endothelia. Neuroimmunomodulation 13, 96–104.
Dutta, R., Trapp, B.D., 2011. Mechanisms of neuronal dysfunction and degeneration in multiple sclerosis. Prog. Neurobiol. 93, 1–12.
Erickson, M.A., Maramara, L.A., Lisman, J., 2010. A single brief burst induces GluR1-dependent associative short-term potentiation: a potential mechanism for short-term memory. J. Cogn. Neurosci. 22, 2530–2540.
Ferrari, C.C. et al., 2004. Reversible Demyelination, Blood-Brain Barrier Breakdown, and Pronounced Neutrophil Recruitment Induced by Chronic IL-1 Expression in the Brain. Am. J Pathol. 165, 1827–1837.
Filippi, M. et al., 1995. Comparison of triple dose versus standard dose gadolinium-DTPA for detection of MRI enhancing lesions in patients with primary progressive multiple sclerosis. J. Neurol. Neurosurg. Psychiatry 59, 540–544.
Foong, J. et al., 1998. Neuropsychological deficits in multiple sclerosis after acute relapse. J. Neurol. Neurosurg. Psychiatry 64, 529–532.
Fox, R.J. et al., 2012. Setting a research agenda for progressive multiple sclerosis: the International Collaborative on Progressive MS. Mult. Scler. 18, 1534–1540.
Frampton, J.E., 2017. Ocrelizumab: first global approval. Drugs 77, 1035–1041.
Fuster, J.M., Alexander, G.E., 1971. Neuron activity related to short-term memory. Science 173, 652–654.
Gacias, M. et al., 2016. Microbiota-driven transcriptional changes in prefrontal cortex override genetic differences in social behavior. Elife 5.
Gardner, C. et al., 2013. Cortical grey matter demyelination can be induced by elevated pro-inflammatory cytokines in the subarachnoid space of MOG-immunized rats. Brain 136, 3596–3608.
Gentile, A. et al., 2016. Interaction between interleukin-1beta and type-1 cannabinoid receptor is involved in anxiety-like behavior in experimental autoimmune encephalomyelitis. J. Neuroinflamm. 13, 231.
Hampton, D.W. et al., 2008. An experimental model of secondary progressive multiple sclerosis that shows regional variation in gliosis, remyelination, axonal and neuronal loss. J. Neuroimmunol. 201–202, 200–211.
Hauser, S.L. et al., 1990. Cytokine accumulations in CSF of multiple sclerosis patients: frequent detection of interleukin-1 and tumor necrosis factor but not interleukin-6. Neurology 40, 1735–1739.
Herges, K. et al., 2012. Protective effect of an elastase inhibitor in a neuromyelitis optica-like disease driven by a peptide of myelin oligodendroglial glycoprotein. Mult. Scler. 18, 398–408.
Hoban, A.E. et al., 2016. Regulation of prefrontal cortex myelination by the microbiota. Transl. Psychiatry 6, e774.
Holmes, C. et al., 2009. Systemic inflammation and disease progression in Alzheimer disease. Neurology 73, 768–774.
Howe, C.L., Mayoral, S., Rodriguez, M., 2006. Activated microglia stimulate transcriptional changes in primary oligodendrocytes via IL-1beta. Neurobiol. Dis. 23, 731–739.
Howell, O.W. et al., 2011. Meningeal inflammation is widespread and linked to cortical pathology in multiple sclerosis. Brain 134, 2755–2771.
Kallaur, A.P. et al., 2016. Cytokine profile in patients with progressive multiple sclerosis and its association with disease progression and disability. Mol. Neurobiol.
Kempuraj, D. et al., 2016. Neuroinflammation induces neurodegeneration. J. Neurol. Neurosurg. Spine 1.
Kitic, M. et al., 2013. Intrastriatal injection of interleukin-1 beta triggers the formation of neuromyelitis optica-like lesions in NMO-IgG seropositive rats. Acta Neuropathol. Commun. 1, 5.
Kjaerby, C. et al., 2016. Serotonin 1B receptors regulate prefrontal function by gating callosal and hippocampal inputs. Cell Rep. 17, 2882–2890.
Klaver, R. et al., 2015. Neuronal and axonal loss in normal-appearing gray matter and subpial lesions in multiple sclerosis. J. Neuropathol. Exp. Neurol. 74, 453–458.
Kreutzberg, G.W., 1996. Microglia: a sensor for pathological events in the CNS. Trends Neurosci. 19, 312–318.
Kutzelnigg, A. et al., 2005. Cortical demyelination and diffuse white matter injury in multiple sclerosis. Brain 128, 2705–2712.
Lagumersindez-Denis, N. et al., 2017. Differential contribution of immune effector mechanisms to cortical demyelination in multiple sclerosis. Acta Neuropathol. 134, 15–34.
Larocque, J.J., Lewis-Peacock, J.A., Postle, B.R., 2014. Multiple neural states of representation in short-term memory? It's a matter of attention. Front. Hum. Neurosci. 8, 5.
Lassmann, H., van Horssen, J., Mahad, D., 2012. Progressive multiple sclerosis: pathology and pathogenesis. Nat. Rev. Neurol. 8, 647–656.
Levesque, S.A. et al., 2016. Myeloid cell transmigration across the CNS vasculature triggers IL-1beta-driven neuroinflammation during autoimmune encephalomyelitis in mice. J. Exp. Med. 213, 929–949.
Litster, B. et al., 2016. Screening tools for anxiety in people with multiple sclerosis: a systematic review. Int. J. MS Care 18, 273–281.
Liu, L. et al., 2010. CXCR2-positive neutrophils are essential for cuprizone-induced demyelination: relevance to multiple sclerosis. Nat. Neurosci. 13, 319–326.

Losy, J., 2013. Is MS an inflammatory or primary degenerative disease? J. Neural. Transm. 120, 1459–1462.
Lublin, F.D. et al., 2014. Defining the clinical course of multiple sclerosis: the 2013 revisions. Neurology 83, 278–286.
Lucchinetti, C.F. et al., 2011. Inflammatory cortical demyelination in early multiple sclerosis. N. Engl. J. Med. 365, 2188–2197.
Magliozzi, R. et al., 2004. Intracerebral expression of CXCL13 and BAFF is accompanied by formation of lymphoid follicle-like structures in the meninges of mice with relapsing experimental autoimmune encephalomyelitis. J. Neuroimmunol. 148, 11–23.
Magliozzi, R. et al., 2007. Meningeal B-cell follicles in secondary progressive multiple sclerosis associate with early onset of disease and severe cortical pathology. Brain 130, 1089–1104.
Mainero, C., Louapre, C., 2015. Meningeal inflammation in multiple sclerosis: the key to the origin of cortical lesions? Neurology 85, 12–13.
Mangiardi, M. et al., 2011. An animal model of cortical and callosal pathology in multiple sclerosis. Brain Pathol. 21, 263–278.
Martinez Yelamos, S. et al., 1999. The social and work-related impact of multiple sclerosis. Neurologia 14, 107–110.
Mashayekhi, F., Salehi, Z., 2016. Administration of vitamin D3 induces CNPase and myelin oligodendrocyte glycoprotein expression in the cerebral cortex of the murine model of cuprizone-induced demyelination. Folia Neuropathol. 54, 259–264.
Merkler, D. et al., 2006. A new focal EAE model of cortical demyelination: multiple sclerosis-like lesions with rapid resolution of inflammation and extensive remyelination. Brain 129, 1972–1983.
Montalban, X., Tintore, M., 2014. Multiple sclerosis in 2013: novel triggers, treatment targets and brain atrophy measures. Nat. Rev. Neurol. 10, 72–73.
Moreno, B. et al., 2011. Systemic inflammation induces axon injury during brain inflammation. Ann. Neurol. 70, 932–942.
Morici, J.F., Bekinschtein, P., Weisstaub, N.V., 2015. Medial prefrontal cortex role in recognition memory in rodents. Behav. Brain Res. 292, 241–251.
Morrow, S.A. et al., 2011. Effects of acute relapses on neuropsychological status in multiple sclerosis patients. J. Neurol. 258, 1603–1608.
Murta, V., Pitossi, F.J., Ferrari, C.C., 2012. CNS response to a second pro-inflammatory event depends on whether the primary demyelinating lesion is active or resolved. Brain Behav. Immun.
Murta, V. et al., 2015. Chronic systemic IL-1beta exacerbates central neuroinflammation independently of the blood-brain barrier integrity. J. Neuroimmunol. 278, 30–43.
Naegele, M., et al., 2011. Neutrophils in multiple sclerosis are characterized by a primed phenotype. J Neuroimmunol.
Nelson, F. et al., 2011. Intracortical lesions by 3T magnetic resonance imaging and correlation with cognitive impairment in multiple sclerosis. Mult. Scler. 17, 1122–1129.
Ontaneda, D., Fox, R.J., 2015. Progressive multiple sclerosis. Curr. Opin. Neurol. 28, 237–243.
Pare, A. et al., 2016. Involvement of the IL-1 system in experimental autoimmune encephalomyelitis and multiple sclerosis: Breaking the vicious cycle between IL-1beta and GM-CSF. Brain. Behav. Immun.
Paxinos, G., Watson, C., 1986. The Rat Brain in Stereotaxic Coordinates. Academic Press, Orlando, FL.
Pelletier, M. et al., 2010. Evidence for a cross-talk between human neutrophils and Th17 cells. Blood 115, 335–343.
Perry, V.H., Linden, R., 1982. Evidence for dendritic competion in the developing retina. Nature 297, 683–685.
Popescu, B.F., Lucchinetti, C.F., 2012. Meningeal and cortical grey matter pathology in multiple sclerosis. BMC Neurol. 12, 11.
Pott Godoy, M.C. et al., 2008. Central and systemic IL-1 exacerbates neurodegeneration and motor symptoms in a model of Parkinson's disease. Brain 131, 1880–1894.
Pott Godoy, M.C., Ferrari, C.C., Pitossi, F.J., 2010. Nigral neurodegeneration triggered by striatal AdIL-1 administration can be exacerbated by systemic IL-1 expression. J. Neuroimmunol. 222, 29–39.
Prut, L., Belzung, C., 2003. The open field as a paradigm to measure the effects of drugs on anxiety-like behaviors: a review. Eur. J. Pharmacol. 463, 3–33.
Pryce, G. et al., 2005. Autoimmune tolerance eliminates relapses but fails to halt progression in a model of multiple sclerosis. J. Neuroimmunol. 165, 41–52.
Ramanujam, R. et al., 2015. Effect of smoking cessation on multiple sclerosis prognosis. JAMA Neurol. 72, 1117–1123.
Ransohoff, R.M., 2006. EAE: pitfalls outweigh virtues of screening potential treatments for multiple sclerosis. Trends Immunol. 27, 167–168.
Rossi, S. et al., 2012. Interleukin-1beta causes synaptic hyperexcitability in multiple sclerosis. Ann. Neurol. 71, 76–83.
Rossi, S. et al., 2014. Interleukin-1beta causes excitotoxic neurodegeneration and multiple sclerosis disease progression by activating the apoptotic protein p53. Mol. Neurodegener. 9, 56.
Scheirer, C.J., Ray, W.S., Hare, N., 1976. The analysis of ranked data derived from completely randomized factorial designs. Biometrics 32, 429–434.
Seppi, D. et al., 2014. Cerebrospinal fluid IL-1beta correlates with cortical pathology load in multiple sclerosis at clinical onset. J. Neuroimmunol. 270, 56–60.
Serafini, B. et al., 2004. Detection of ectopic B-cell follicles with germinal centers in the meninges of patients with secondary progressive multiple sclerosis. Brain Pathol. 14, 164–174.
Serres, S. et al., 2013. Magnetic resonance imaging reveals therapeutic effects of interferon-beta on cytokine-induced reactivation of rat model of multiple sclerosis. J. Cereb. Blood Flow Metab. 33, 744–753.
Shimommura, Y. et al., 1990. Effects of peripheral administration of recombinant human interleukin-1 beta on feeding behavior of the rat. Life Sci. 47, 2185–2192.
Silver, N.C. et al., 2001. Quantitative contrast-enhanced magnetic resonance imaging to evaluate blood-brain barrier integrity in multiple sclerosis: a preliminary study. Mult. Scler. 7, 75–82.
Soulika, A.M. et al., 2009. Initiation and progression of axonopathy in experimental autoimmune encephalomyelitis. J. Neurosci. 29, 14965–14979.
Stassart, R.M. et al., 2015. A new targeted model of experimental autoimmune encephalomyelitis in the common marmoset. Brain Pathol.
Swiergiel, A.H., Dunn, A.J., 2007. Effects of interleukin-1beta and lipopolysaccharide on behavior of mice in the elevated plus-maze and open field tests. Pharmacol. Biochem. Behav. 86, 651–659.
Tambalo, S. et al., 2015. Functional magnetic resonance imaging of rats with experimental autoimmune encephalomyelitis reveals brain cortex remodeling. J. Neurosci. 35, 10088–10100.
Teeling, J.L., Perry, V.H., 2009. Systemic infection and inflammation in acute CNS injury and chronic neurodegeneration: underlying mechanisms. Neuroscience 158, 1062–1073.
Tsukada, N. et al., 1991. Tumor necrosis factor and interleukin-1 in the CSF and sera of patients with multiple sclerosis. J. Neurol. Sci. 104, 230–234.
Ucal, M. et al., 2017. Widespread cortical demyelination of both hemispheres can be induced by injection of pro-inflammatory cytokines via an implanted catheter in the cortex of MOG-immunized rats. Exp. Neurol. 294, 32–44.
Valentin-Torres, A. et al., 2016. Sustained TNF production by central nervous system infiltrating macrophages promotes progressive autoimmune encephalomyelitis. J. Neuroinflamm. 13, 46.
Watzlawik, J., Warrington, A.E., Rodriguez, M., 2010. Importance of oligodendrocyte protection, BBB breakdown and inflammation for remyelination. Expert Rev. Neurother. 10, 441–457.
Wu, F. et al., 2010. Extensive infiltration of neutrophils in the acute phase of experimental autoimmune encephalomyelitis in C57BL/6 mice. Histochem Cell Biol. 133, 313–322.
Zeis, T. et al., 2008. Normal-appearing white matter in multiple sclerosis is in a subtle balance between inflammation and neuroprotection. Brain 131, 288–303.
Zivadinov, R., Pirko, I., 2012. Advances in understanding gray matter pathology in multiple sclerosis: Are we ready to redefine disease pathogenesis? BMC Neurol. 12, 9.